42nd Turbomachinery
29th Pump SYMPOSIA

Proceedings of the Forty-Second Turbomachinery Symposium
October 1- 3, 2013, Houston, Texas

# HISTORY OF EVOLUTION, PROGRESS AND APPLICATION OF SAFE DIAGRAM FOR TUNED AND MISTUNED SYSTEMS

Murari Singh, Ph.D

Safe Technical Solutions, Inc
4430 Loraine Lane, Suite 100
Bethlehem, PA 18017

**Dr. Murari Singh** (Bethlehem, Pennsylvania) is the President of Safe Technical Solutions, Inc (SAFETSOL). Dr. Singh has been involved in the design, development and analysis of industrial turbo machinery for forty years with Turbodyne Corporation, Dresser Industries, Dresser-Rand Company, and GE CONMEC and most recently with GE Oil & Gas as Consulting Engineer. Dr. Singh has extensive knowledge and experience with fatigue and fracture mechanics, stress and vibration of structures, reliability, life analysis, probabilistic analysis. His practical application experience includes a variety of rotating equipments including CAES, Warm Gas and FCC Expanders, Steam Turbines, Gas Turbines and Centrifugal and Axial Compressors. He developed the widely used SAFE diagram for reliability evaluation of turbine blades. The SAFE diagram methodology is superior to other methods in providing clear analytical and predictive information. This concept has been applied to other turbo machineries. It is considered to be a significant contribution to design methods and vibration technology for the evaluation of blade reliability. Dr. Singh has been involved in (developing and teaching) application of lifing strategy to many mechanical components. This includes subjects dealing with hcf, lcf, creep, and fracture mechanics. Probabilistic method is used to estimate risk in design. He authored many technical papers and he is the co-author of the books *"Steam Turbine, Design, Application, and Rerating"*, second edition and *"Blade Design and Analysis for Steam Turbines"*. He is co-authoring a book on *"Expander for Oil & Gas"* to be published by McGraw-Hill Company.

## ABSTRACT

Concept of Safe diagram was introduced 30 years ago (Singh and Schiffer, 1982) for the analysis of the vibration characteristics of packeted bladed disc for steam turbines. A detailed description of Safe diagram for steam turbine blades was presented 25 years ago in the 17th Turbo Symposium (Singh et. el, 1988). Since that time it has found application in the design and failure analysis of many turbo machineries e.g. steam turbines, centrifugal compressor, axial compressor, expanders etc. The theory was justified using the argument of natural modes of vibration containing single harmonics and alternating forcing represented by pure sine wave around 360 degrees applied to bladed disk. This case is referred as tuned system. It was also explained that packeted bladed disc is a mistuned system where geometrical symmetry is broken deliberately by breaking the shroud in many places. This is a normal practice which provides blade packets design. This is known as deliberate geometrical mistuning. This mistuning gave rise to frequency of certain modes being split in two different modes which otherwise existed in duplicate. Natural modes of this type construction exhibited impurity i.e. it contained many harmonics in place of just one as it occurs in a tuned case. As a result, this phenomenon gives rise to different system response for each split mode. Throughout the years that have passed, Safe diagram has been used for any mistuned system- random, known or deliberate.

Many co-workers and friends have asked me to write the history of the evolution and of the first application of this concept and its application in more general case. This paper describes application of Safe diagram for general case of tuned system and mistuned system.

## INTRODUCTION

Vibration-related blade and disc failure in turbo machinery due to resonant excitation is a common phenomenon. The resulting damage to blades and disc is due to high cycle fatigue. At resonant excitation the dynamic stress amplitudes increases as the exciting frequency approaches the resonant speed and the response decreases after passing through the resonant speed. Hence, the design decision is dependent upon the identification and avoidance of resonant frequencies of the system.

As operators and manufacturers gained experience, new technical methods and lessons learned from field experience have been included in the design decision making process. In turn, each manufacturer has evolved its own process and criteria to achieve successful design.

Estimation of the resonance characteristics of blades is a multi-discipline activity. Information is needed about unsteady aerodynamics over a wide variety of flow conditions that may exist within the operating range and structural vibration characteristics, i.e., frequencies and associated mode shapes within the operating range; damping in the system (structural as well as aerodynamic). Estimation or actual material properties (fatigue properties, yield strength, ultimate strength, modulus of elasticity, etc.) at the temperature in the operating range should be available. Manufacturing and quality assurance processes should be well defined and followed. Each of these issues may require a separate technical discipline to support an evaluation.

This paper includes a brief history of the evolution of Safe diagram for a perfectly tuned system. Mathematical expression for work done by the alternating force on the vibrating system that forms the basis of Safe diagram is presented. It shows the expected response of perfectly tuned system and mistuned system. It also explains the application of Safe diagram for mistuned system (geometrical variation, forcing distortion), split modes/localized modes, deliberate mistuning (packeting-odd and even number of blades), random mistuning (geometry and forcing) and it also includes effect of centrifugal stiffening. Examples are included from many published papers.

## HISTORY OF EVOLUTION OF SAFE DIAGRAM

Vibration analysis of steam turbine blade design has progressed from the analysis of blade as spring mass systems to single cantilever beam to packet of blades to bladed disk as a system. Effects of turbine speed to increase blade frequency were found and it gave rise to the term "centrifugal stiffening". Campbell (1924), while examining the failure (bursting) of disks, concluded that blades were broken due to axial vibration. The results of an investigation to understand the wheel failures, mostly in wheels of large diameter that could not be explained on the basis of high stress alone were presented. This test was conducted by scattering sand over the wheel surface. Frequency of excitation was varied until a sand pattern on the wheel appeared and sand accumulated mostly in radial lines or patterns. When the frequency changed to some higher magnitude a different sand pattern appeared on the wheel. These radial lines represented the location where velocity of vibration was zero. The number of radial lines was always observed to be of an even number. These patterns are known as nodal patterns and two radial lines are taken as one diameter. It is now understood that the opposite radial lines in each instance might not be 180 degrees apart. This is a sign of impure mode containing multiple harmonics. Frequencies at which these patterns are observed coincide with the natural frequency of the wheel in axial vibration associated with the mode shape represented by the sand pattern.

There are six (6) radial lines in the pattern shown in Fig. 1. These modes are called three (3) nodal diameters mode. It should be noted that the radial lines pass through the balancing holes in the left picture while in the picture on right side these lines pass between the balancing holes. This shows that there are two natural modes having same nodal diameters. This is the case of splitting of the modes due to broken symmetry and the frequencies of these modes may be different. This is a case of deliberate mistuning which will be explained later.

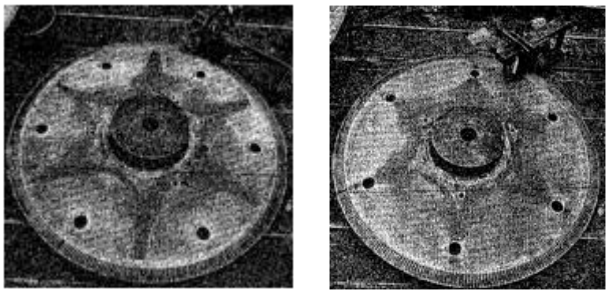

Figure 1 Six Radial Lines, Three Nodal Diameters Modes (Campbell 1924)

Blade damage problems in steam turbines were encountered during WWII. With the help of computers that was capable to handle large calculations, Weaver and Prohl (1956) demonstrated that blades in the band behave differently than single blade. They showed that there were more frequencies and mode shapes of banded construction compared to what the analysis of a single blade provided. The response of blades under excitation due to flow from nozzle, natural frequencies of the banded blades and also the associated mode shapes were evaluated. In a companion paper Prohl (1956) described the numerical method and provided the equations that were used to estimate frequencies, mode shapes and dynamic response of the banded blades. The basic beam equations for blades were developed where blades were coupled together through a band at the tip of the blades. Disk was not included in the analysis. Stimulus was assumed to be uniformly distributed along the length of the blade. The phase between stimulus and blade motion is constant along the length of the blade. Fig. 2 summarizes the results of the analysis for vibrations for seven modes. The first six tangential modes are considered to belong to the first bending of a single blade and the difference among them is the phasing among blades. The seventh mode is the second tangential mode in which there is a phase change along the length of the blade.

The analytical result for the dynamic response of blades was found to be a function of the (a) number of harmonic excitation, (b) number of nozzle openings and (c) number of blades per 360 degrees. The shapes of these curves, which resemble that created by a "bouncing ball", are functions of mode shapes of the blade group. Blades were analyzed as a group rather than a single blade that was practice before this publication. The dynamic response of the group is due to the coupling between blades through the shroud band. Frequency is a function of the relative stiffness of the band and the blade.

The resonant response is affected by the nozzle pitch, blade pitch and the number of blades in each packet. The review of Fig. 2 and Fig. 3 indicates that with a proper selection of nozzle and blade pitching, it may be possible to considerably reduce the resonant stress even though operating precisely at the speed required to excite the natural frequency.

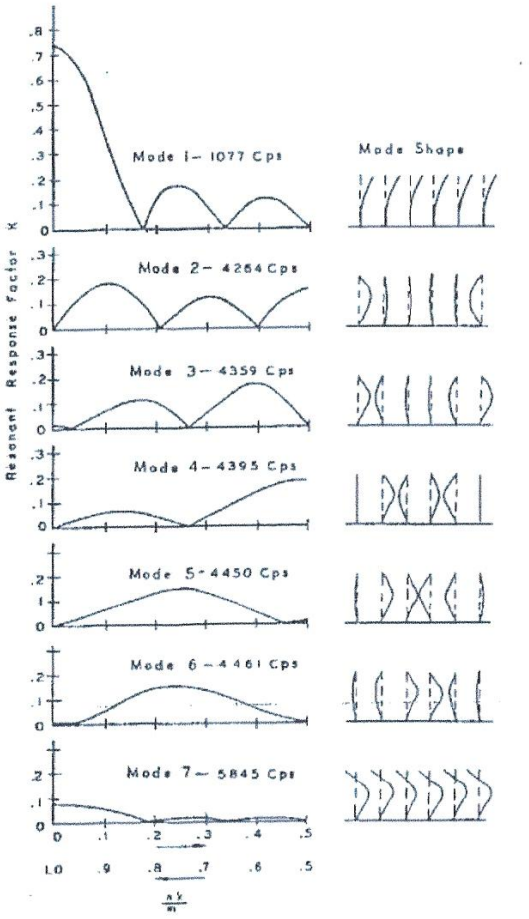


Figure 2 Resonant Response Factor (Weaver and Prohl, 1958).

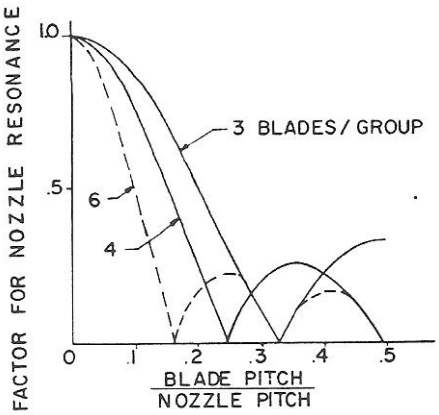


Figure 3 Bouncing ball (Weaver and Prohl, 1958).

In the discussion section of Weaver and Prohl (1956) paper, D.D. Rosard pointed out that resonant peak decreases as the number of blades in a packet is increased and the peak occurs at different ratio of blade pitch to nozzle pitch. It is evident from Figure 3 which he provided.

Results of this work provided the future direction for analysis of banded group of blades. This was a milestone in the analytical development of blade vibration and decision making process for reliability.

At this time, Johnson and Bishop (1956) presented analytical results of important system with equal frequencies and is shown in Fig. 4. They considered a system consisting of a single mass, M, to which n equal masses, m have been attached through springs of equal stiffness, k. Each mass has one degree of freedom, which is in the vertical direction. This system resembles a bladed disk system as used in turbines, which will help to understand its behavior. Mass M is that of a disk with infinite stiffness and grounded by spring stiffness, $x_0$. Small mass m represents the mass of the blade and blade's stiffness is k. The results of this analysis have shown that there are a number of equal natural frequencies in this type of system but the natural mode shapes will be different. Many frequencies had same mode shapes but these differed by a phase difference. The total number of degrees of freedom for this system is equal to the number of masses and is equal to (n+1). Therefore, there will also be (n+1) natural frequencies.

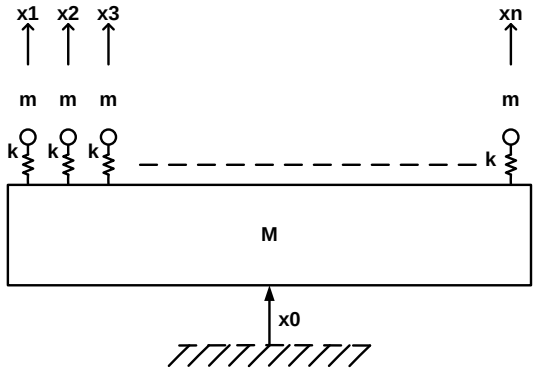


Figure 4 Systems with Equal Mass and Stiffness

It was recognized that a bladed disk is a system and coupling between blades will also be through the disk. Consideration of the stiffness of the disk became important as earlier found also by Campbell (1924). In the tangential vibration of blades, stiffness of the disk may be considered very high, but the coupling between blades will be small. Johnson and Bishop's analysis resembles a bladed disc in tangential vibration. However, in the axial vibration, disk stiffness becomes a large contributor.

Including geometrical variations among blades was considered next in the analysis of the dynamic response of blades. It has been shown that geometrical variations influences mode shapes and frequencies and in turn, the response of a bladed disk system. In a tuned system where each blade is identical, modes occur in duplicate. There are two modes that differ by a phase angle but these modes have identical

frequencies. However, when symmetry is disturbed through variation from blade to blade or any other geometrical variation, some modes split in two frequencies. Also, the shape of these modes get distorted from the tuned case, which is a phenomenon called "mistuning". Paper by Ewins (1969) contains an extensive discussion of this phenomenon. The response of the mistuned case was found to occur at slightly different frequency from the tuned case. Amplitude was attributed mainly due to a change in the mode shape and the shift in frequency was due to splitting of the mode. This posed a serious decision point for designers to account for variability among blades. Ewins (1975) specifically dealt with completely shrouded or un-shrouded bladed disk constructions.

At this time there was no publication that reported the results of a packeted bladed disk analysis. The next stage of advancement occurred in the analysis of disks containing packets of blades. This analysis in a way merged the concept of Campbell (1924) and Weaver and Prohl (1956). The blades of steam turbines more often are banded together in a packet. Singh (1982, 1988 and 1989) studied the dynamic behavior of packeted bladed disk construction. Results of these analyses led to the introduction of Safe diagram. In case of axial vibration, Fig. 5 shows a comparison of a Safe (**S**ingh's **A**dvanced **F**requency **E**valuation) diagram for different types of construction for the same number of blades mounted on the same disk. The vibration characteristic of packeted bladed disks is similar to the completely bladed disk but it has some special features of split modes. In case of bladed disc with cantilevered single blade and cantilevered blade packet frequencies are shown as horizontal lines on Safe diagram. Reason of this is that frequency remains constant but mode shapes also may be designated as nodal diameters due to phasing between blades.
The Safe diagram for cantilevered conditions is the upper limit of appropriate constructions whether it is free standing bladed disc design or completely shrouded bladed disc design.

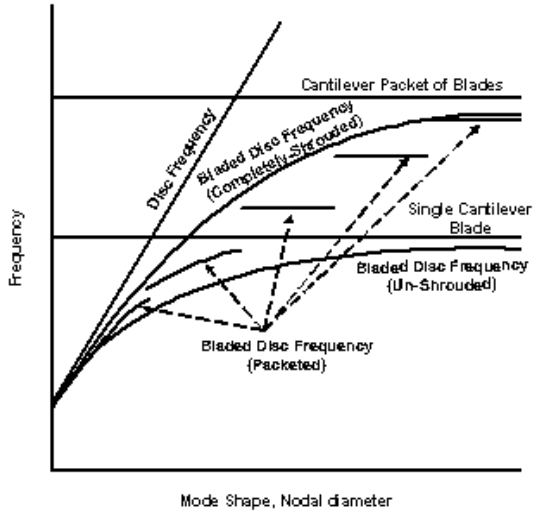


Figure 5 Safe diagrams for Completely Shrouded, Un-shrouded and Packeted Bladed Disk (Singh and Drosjack, 2008)

For the development of Safe diagram there were two main considerations. First, during mid 1970 while employed at Turbodyne Corporation, Wellsville, a customer (Late Cliff Cook) requested to examine and to explain the results of the paper published by Provanzale and Skok (1973). My supervisor (Late Howard Vreeland) asked me to discuss this issue with the customer. The existing method of analysis at the time for banded blades was to consider it as a group but cantilever at the base where it connected to the disk. The results of this analysis conformed to the findings of Weaver and Prohl (1956). Second, to understand the full implication of Provanzale's paper, I was visiting the laboratory and the test engineer (Mr. Steve Todd) caught hold of me to show the results of the TFA (Transfer Function Analysis) test that he was conducting on a complete packeted bladed disk. While examining the mode shapes at many frequencies we noticed that many frequencies were exhibiting basically the same natural mode shapes of any packet of blades, mostly for the axial modes Fig. 6. Some tangential modes of the same shape showed up at different frequencies which did not conform to the results of Weaver and Prohl (1956). Phasing between blades of each packet was the same but the phasing between packets was observed to be different for different modes. It became clear that there was something missing in the analysis, most importantly between packets. This pointed towards including disk flexibility (stiffness) in the analysis.

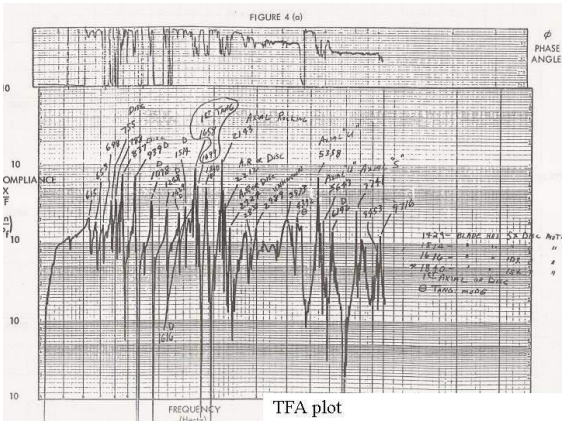


TFA plot

Figure 6 A Representative TFA Plot of a Packeted Bladed Disk

It was decided to analyze a complete packeted bladed disk with impulse blades using finite element method (FEM). Impulse blade was used to eliminate the coupling between axial and tangential modes of vibration of blades and to better understand both tangential and axial vibration. This resulted in the understanding of the vibration behavior of packeted bladed disk. First application of this finding was used to solve a blade failure in a four stage turbine. Results of this analysis for tangential modes of vibration were first reported by Singh in 1980 in ASME conference and this was published by Singh and Schiffer (1982). To understand the physics of this behavior a mathematical expression of the work done by the alternating force applied to any mode shape at a frequency was examined. This revealed the importance of considering natural mode

shape and the shape of the applied force in estimating the response of the system. Brief description of the mathematical treatment is included in the paper that is the base of response of tuned as well as mistuned system.

This exercise gave rise to two conditions for pure resonance where response of the system might be uncontrolled for very low damping.

The following two conditions are for a true resonance to occur:

1. The frequency of the exciting force equals the natural frequency of vibration, and
2. The profile (shape) of the applied force has the same shape as the mode shape associated with that natural frequency.

Above statements are true for tuned case as well as mistuned case. For mistuned system either it might be case of forced response or due to splitting of frequency there will be high response at a frequency where it might have been low or no response at all. The mathematical expression for the work done confirms this statement.

## *Mathematical Expression for work done by exciting force*

### *Tuned System*

Mathematical expressions for work done by alternating force provided support that each of the conditions for resonance to occur is necessary, but neither is sufficient by itself. The time varying periodic forces experienced by rotating blades can be resolved in harmonics. It is accomplished by performing Fourier decomposition of the periodic force shape. The frequencies of the harmonics are an integer multiple of the speed of rotation. In general, the force experienced by the blades of a turbine disc during a complete revolution is the consequence of any circumferential distortion in the flow field.

The frequency of the excitation due to nozzle vanes, struts, or any obstruction in the flow field as a function of rotational speed and number of obstruction is given by:

$$\omega_K = (K.N)/60 \qquad (1)$$

Where

$\omega_K$ = frequency of the exciting force, Hz
K = number of distortions in the flow per $360^0$, e.g., number of nozzles, or number of struts in the flow field, etc.
N = turbine speed, RPM

K represents the shape of the excitation and it is denoted as k nodal diameter. The spacing of the obstruction is assumed to be symmetrical. The nozzle passing excitation occurs exactly at the multiple of nozzle counts. The magnitude of excitation decreases with increasing multiple of harmonics. This is the case of a tuned system. This is true when there is no variation between nozzles otherwise there will be harmonics other than multiple of nozzle counts in the shapes. Therefore, $K_{th}$ harmonic of the force applied to the blades for tuned case is written as the following:

$$P_k(\theta, t) = P_k \, Sin(\omega_K t + K\theta) \qquad (2)$$

Where the frequency of the force is $\omega_k$ and $\theta$ is the angle on the disc from a reference point.

The mode shape with m nodal diameters and the natural frequency ($\omega_m$) is expressed as the following:

$$\underline{X_m}(\theta, t) = -A_m Cos(\omega_m t + m\theta) \qquad (3)$$

Again, it is assumed that the mode shape contains only one harmonic i.e. structurally it is a tuned system. The condition of resonance can occur when the alternating force does positive work on the blade.

*Work done by an applied force*

The work done by the $k_{th}$ harmonic of the force acting on m nodal diameters mode shape in one complete period, T, is expressed as follows:

$$W = \int_0^{2\pi}\int_0^{T} P_k(\theta, t)\ \frac{d}{dt} X_m(\theta, t)\ \frac{N}{2\pi}\, dt\, d\theta$$

$$= \int_0^{2\pi}\int_0^{T} P_k \, Sin(\omega_K t + K\theta)\ \omega m A_m Sin(\omega_m t + m\theta)\ \frac{N}{2\pi}\, dt\, d\theta \qquad (4)$$

$$= N\pi P_k A_m \quad (\text{for } m = K \text{ and } \omega_m = \omega_K)$$

Or

$$= 0 \quad (\text{For either } m \neq K \text{ and/or } \omega_m \neq \omega_K) \qquad (5)$$

The first expression of equation 5 is the positive work ($N\pi P_k A_m$) done by the force. This is true only if the nodal diameter, m, of the mode shape is the same as the shape of the $k_{th}$ harmonic of the force and the natural frequency ($\omega_m$) of vibration is equal to the frequency, $\omega_K$, of the force.

Zero work results when either the nodal diameter, m, of the mode shape is not the same as the shape of the $k_{th}$ harmonic of the force or the natural frequency, $\omega_m$, of vibration is not equal to the frequency, $\omega_K$, of the force. This is the basis of the Safe diagram and it further explains the need to examine the frequency of vibration, the mode shape and the shape of the force when considering resonance. The two conditions mentioned earlier are the statement of the above mathematical expression for the work done.

*Mathematical Expression of Work done for Mistuned System*

The mode shape for a mistuned system gets distorted depending on the type and amount of mistuning whether it is deliberate or random. Packeted bladed disk, balance holes in the disk, odd numbers of blades on a disk or missing blade space for closing are examples of deliberate mistuning. Random mistuning may occur due to manufacturing tolerance of the blades. Blades may be within specified tolerance but each blade may be different, if they are not individually measured or assembled randomly on the disk. In these cases mode shapes are distorted and certain mode might contain many harmonics. This mode may also split in two frequencies. It was found in the case of packeted bladed disk that even in such a situation contribution of a particular harmonics will be largest. For plotting Safe diagram this has been named after that harmonic with understanding there may be other harmonics in the shape.

*Expression for work done for a tuned bladed disk*

The general expression for any one of the split mode shape can be written as

$$X(M) = \Sigma A_L \sin(L\theta + \varphi_L) \quad (6)$$

Where L is the half of the number of blades (N) for even number of blades or (N-1)/2 for odd number of blades on the disk

In general case when forcing is also mistuned then the shape of the force can be expressed as follows:

$$F(N) = \Sigma F_L \sin(L\theta + \phi_L) \quad (7)$$

$$dW = F(N).d(X(M))$$

The complete expression for dW is given in the Appendix.

Using the complete integral relationship, the final expression for work done is given by the following:

$$W = \pi (2A_0F_0 + A_1F_1 \cos\varphi_1 \cos\phi_1 + 2A_2F_2 \cos\varphi_2 \cos\phi_2 + 3A_3F_3 \cos\varphi_3 \cos\phi_3 + \ldots\ldots + LA_L F_L \cos\varphi_L \cos\phi_L) \quad (8)$$

The following conclusions can be drawn:

1. The blade will respond to the harmonics of force that match with the harmonic contents of the mode shape.
2. The resulting response distribution may be different than the mode shape.
3. It is quite possible that there will not be a true resonance, but a forced response in a mistuned system.

Any natural mode of a bladed disk is represented by three parameters, namely, frequency, its shape and any variation of frequency (if any) due to speed. The forcing function as represented by Equation 1 contains the same three variables, frequency, shape and speed. It became clear that modes and forcing harmonics are three dimensional surfaces. A 3 dimensional physical model was made consisting of wood and plexi glass panel in early 1980's to demonstrate that the bladed disk vibration may be represented by this model Fig 7.

Figure 7 Physical 3 D Wooden Model (Courtesy: Terryl Mathews)

Modes and harmonics of force were represented by different color threads. The mode lines and the force harmonic lines crossed each other. Examination of these points it was evident that the locus of these points is a three dimensional curve. It became clear that a graphical representation is also required to show this feature.

To explain the findings of this model, Singh and Schiffer (1982) reported in detail thru graphical presentation for completely shrouded and for packeted bladed disk. Any natural mode of a bladed disk is represented by three parameters, namely, frequency, its shape and any variation of frequency (if any) due to speed. Fig. 8 is a 3D representation.

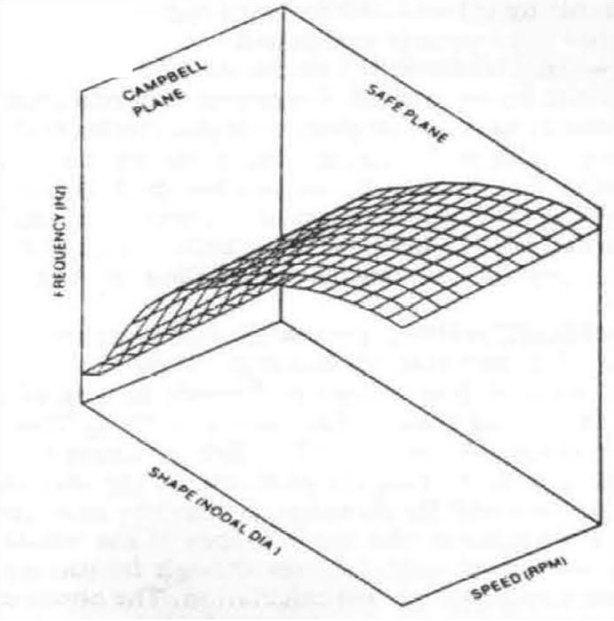


Figure 8 3D Representation of Vibration Characteristic of a Bladed Disc (completely shrouded or free standing)

The forcing function is graphically shown in Fig. 9.

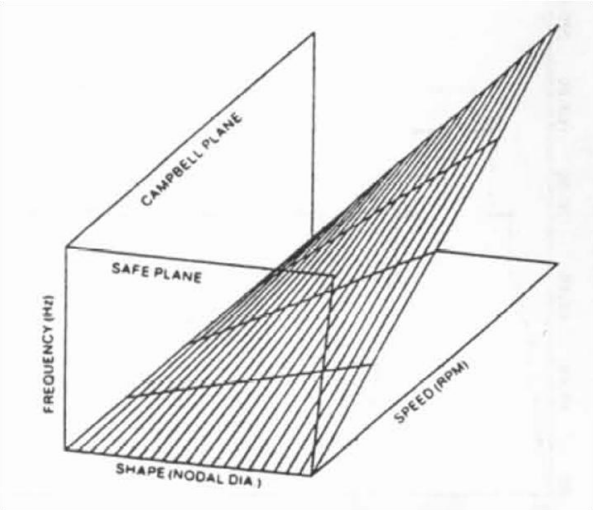


Figure 9 3D Representation of Force Excitation

The probable points of resonance are found by superimposing Fig. 8 and Fig. 9.

The points of intersection and its locus will be a 3D curve since these two intersecting surfaces are three dimensional. Three planar views (two vertical and one horizontal) of these points for a 40 bladed disc are shown in Figs. 10 through 12. These are the resonance points, which satisfy equation 5. Frequencies are equal at these points, as well as, the mode shape is identical to the shape of the force.

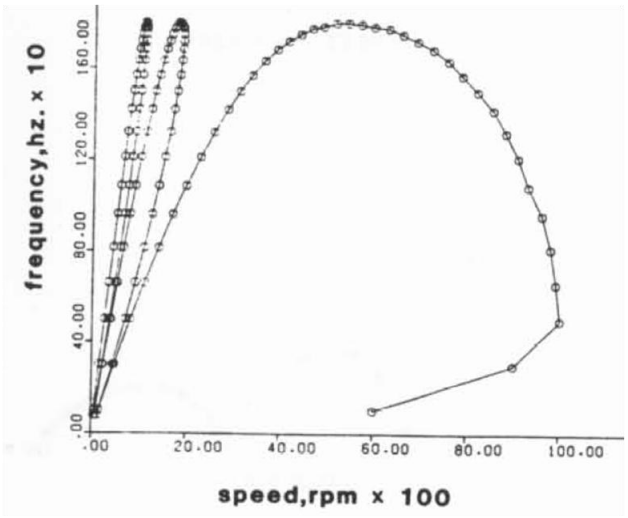


Figure 10 Projection of Resonance Points on the Campbell Plane (completely shrouded or free standing blades)

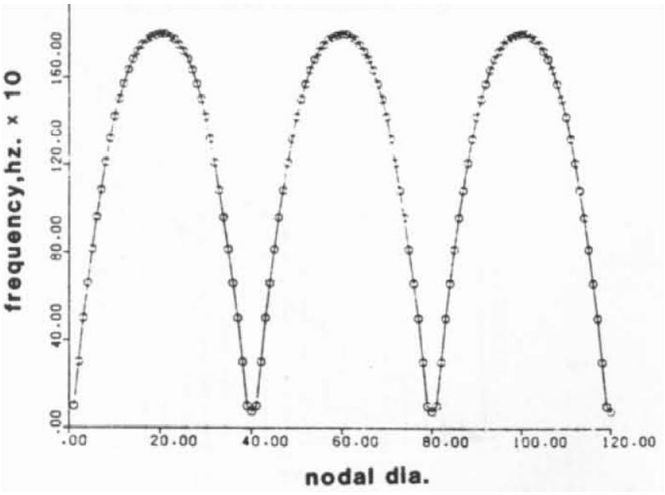


Figure 11 Projection of Resonance Points on the Safe Plane (completely shrouded or free standing blades, 40 blades)

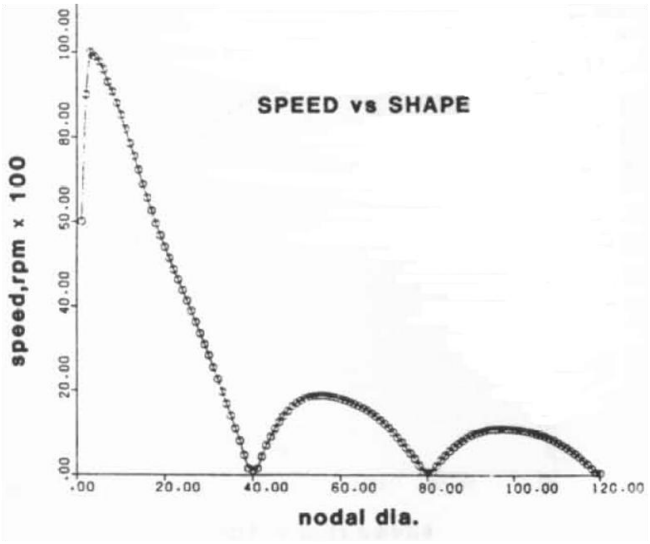


Figure 12 Projection of Resonance Points on the Horizontal Plane (completely shrouded or free standing blades)

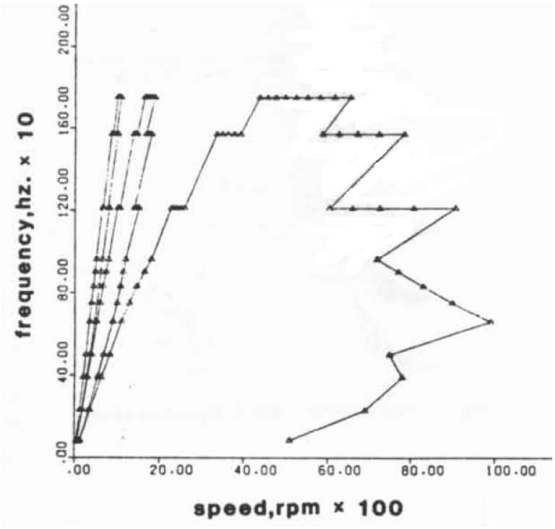


Figure 13 Projection of Resonance Points on the Campbell Plane (packeted bladed disc)

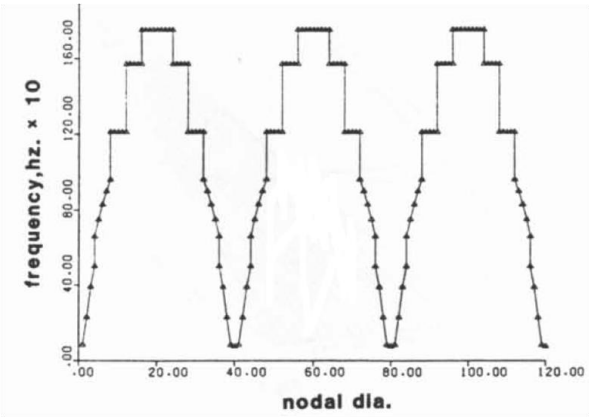


Figure 14 Projection of Resonance Points on the Safe Plane (packeted bladed disc, 40 blades)

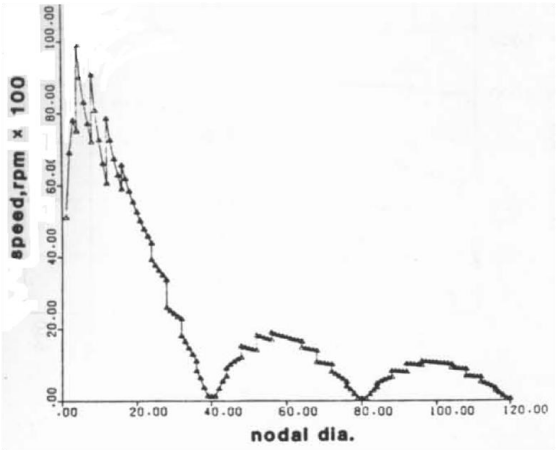


Figure 15 Projection of Resonance Points on the Horizontal Plane (packeted bladed disc)

Also the plots for resonance points for a packeted bladed disc assembly are shown in Figs. 13 through 15.

The first vertical plot represents the plane of Campbell diagram. The second vertical plot is the Safe plane where the horizontal axis represents shape and the vertical axis represents frequency. Inspection of Figs. 10 through 15 reveals that the projection of intersection points on the Safe plane shows a remarkable symmetry and repeatability. Plot on the Safe plane from zero through 20 ND contains all resonance points. It is easier to construct and represent these points on the Safe diagram as it will become clear later for any order of excitation.

The Safe diagram combines natural frequencies, mode shapes, excitation frequencies and the shape of the force, and operating speeds on one graph. It has been found to be an excellent guide to determine the potential of exciting a particular mode of vibration. For a circular system, these points fall on radii (always an even number) or circles. A pair of radii (often opposite each other) is considered as a diameter. Mode shapes is specified by the number of nodal diameters (ND) and nodal circles (NC). The x-axis of the diagram represents nodal diameters and the frequency is plotted on the y-axis of the interference diagram.

**NAMING SAFE DIAGRAM**

To name this diagram, a contest was initiated by the President of Steam turbine Division of Dresser-Rand, Wellsville. Two names were on the top of the list namely "Singh's Strings" and "Safe diagram". Second name was finally chosen to stand for "**S**ingh's **A**dvance **F**requency **E**valuation". Fig. 16 is the photograph of the base of the model that was given to Late Charley Ramsey of Dow Chemical Company and it is now with Terryl Mathews of Shell who was kind enough to provide with photographs of the original model.


Figure 16 Photograph of the Base of the Model (Courtesy: Terryl Mathews)

Description of the resonance re: coincidence of frequencies and shapes was so clear that Dresser-Rand decided to build

small models for distribution to customers. Photographs of this models are given in Figure 17.

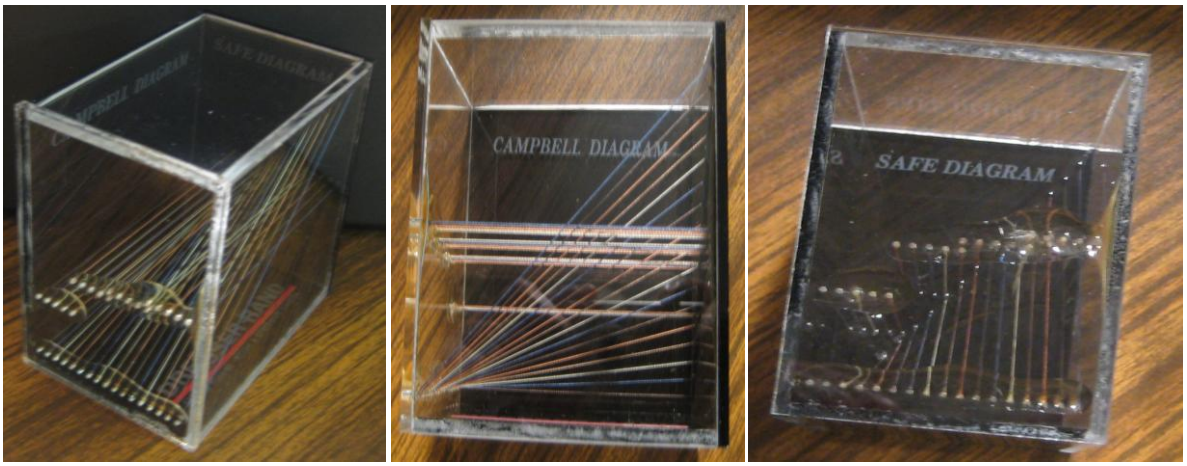


Figure 17 3 D Small Model Representation of Campbell and Safe diagrams

It was found that Safe diagram can estimate the possibility of unreliability in a manner that is simpler than those obtained after much analysis as presented by Weaver and Prohl. Weaver and Prohl used energy method to calculate response of a 192 bladed disk. The disk was composed of 32 packets with 6 blades in each packet. The number of nozzles ahead of the stage was 92. Also, Singh and Vargo (1989) were able to show that the results presented by Provanzale and Skok (1973) can be explained based on Safe diagram, which provides a better explanation of the response points. This development led to the explanation of the paper presented by Provanzale and Skok and it included the effect of coupling provided by disk and shroud band.

Fig. 18 and Fig. 19 show the comparison of Singh's analysis with that presented by Provanzale and Skok. This comparison convinced us that our approach is sound and easier. We explained the findings to the customer to his satisfaction.

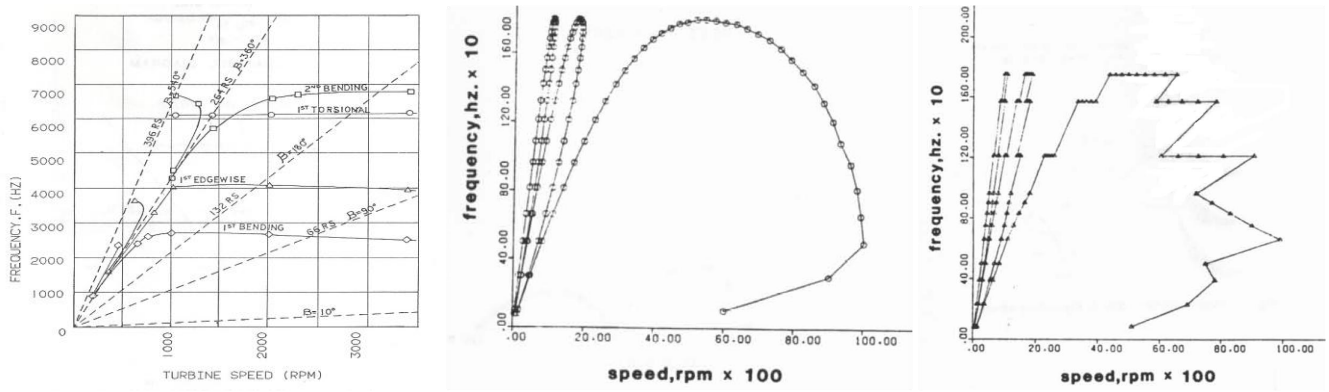


Figure 18 Resonance points on Campbell Plane

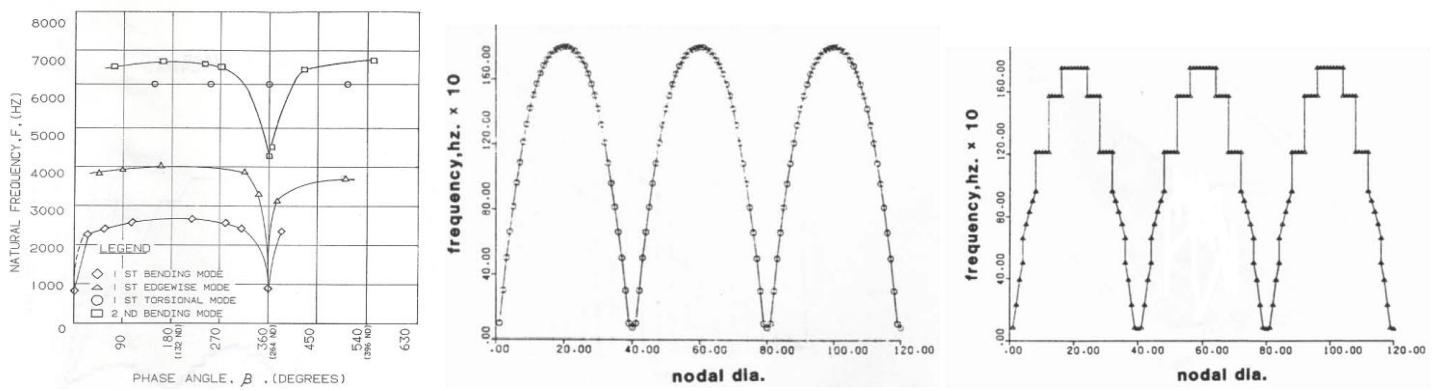


Figure 19 Resonance points on Safe Plane

Safe diagram, which combines natural frequencies, mode shapes, excitation frequencies, and operating speeds on one graph, is found to be an excellent guide in determining the possibility of exciting a particular mode of vibration. In any vibration cycle, certain parts of a mechanical structure remain stationary. For a circular symmetric system, these points fall on radii (always an even number) or circles. A pair of radii (opposite each other) is considered as a diameter. Mode shapes can be characterized by specifying the number of nodal diameters (ND) and nodal circles (NC). The x-axis of the diagram represents nodal diameters. Frequency is plotted on the y-axis of the Safe diagram. A good design would yield a Safe diagram that indicates no coincidence of possible excitation force with a natural mode of a bladed disc or an impeller (tuned system).

## FIRST APPLICATION OF SAFE DIAGRAM

Just at this time, one stage of a four stage turbine was experiencing blade damage during operation. The Campbell diagram of the stage is given in Fig. 20. It showed that there is a possibility of resonance of one of the tangential modes with 1xNPF excitation. Primary axial modes were not in resonance with 1xNPF. This type of design had been used before because the stresses were low and experience with this design had been very encouraging. Finite element modal analysis was conducted at this time to confirm the previously obtained results. Safe diagram were plotted first time by hand on a graph paper. Figure 21 and Figure 22 show the Safe diagram for tangential and axial modes respectively. Safe diagram confirmed the findings of Campbell diagram. A mode belonging to tangential fixed supported mode coincided with 1xNPF excitation. Modification was made to the design of this stage by changing blade profile and number of blades. There was a mixed packeting of some six blades and five blades in packets. Campbell diagrams are shown in Figure 24 and Figure 25 respectively. Moreover, stresses were within acceptable limits. Safe diagram of the modified design is shown in Figure 26 and Figure 27. Campbell and Safe diagrams showed that this design is acceptable for operation.

The question was raised that Safe diagram had only confirmed the findings of Campbell diagram. Then what is the added value of Safe diagram? As it happened that another stage of the same turbine had very similar Campbell diagram. Safe diagram was plotted for this stage. While Campbell diagram was indicating a possibility of resonance, Safe diagram was clean indicating no possibility of resonance. This stage has not experienced any damage of the blade. Results and conclusions of this finding are included in the paper by Singh and Schiffer (1982). Most important conclusion that could be drawn is that if Safe diagram shows resonance then Campbell diagram will also show resonance. On the other hand if Safe diagram shows no possible resonance, Campbell diagram might show resonance.

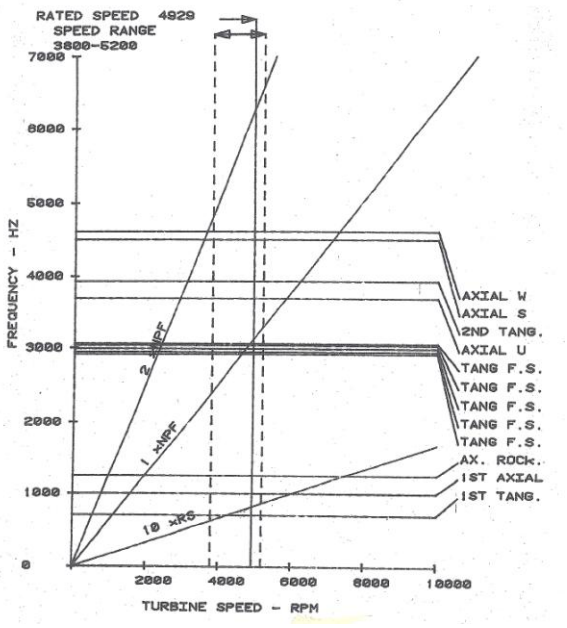


Figure 20 Campbell diagram for Original Design

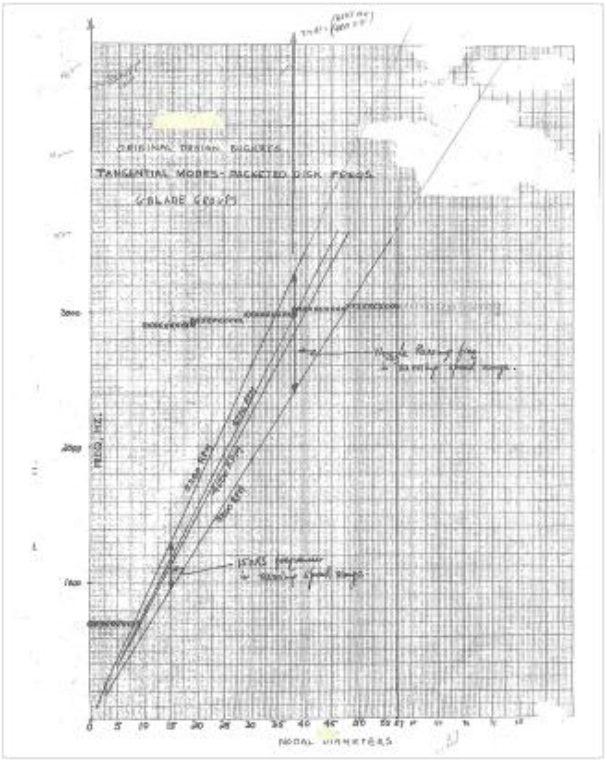

Figure 21 safe diagrams for Original Design (Tangential Modes)

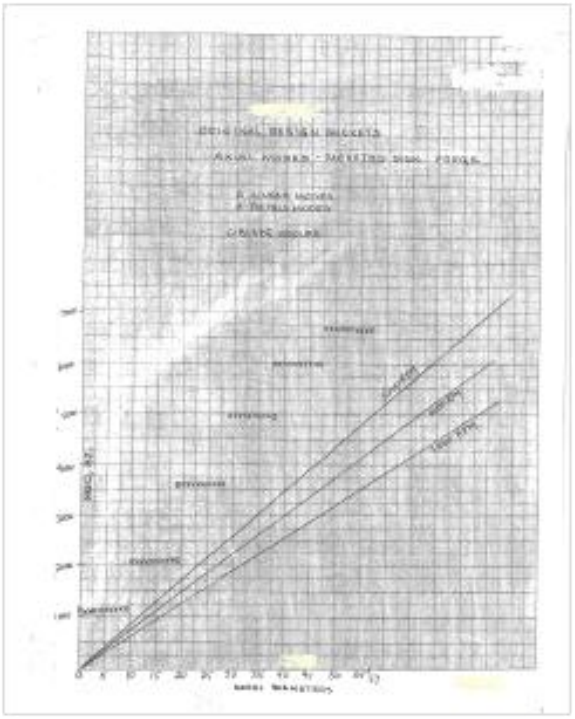

Figure 22 safe diagrams for Original Design (Axial Modes)

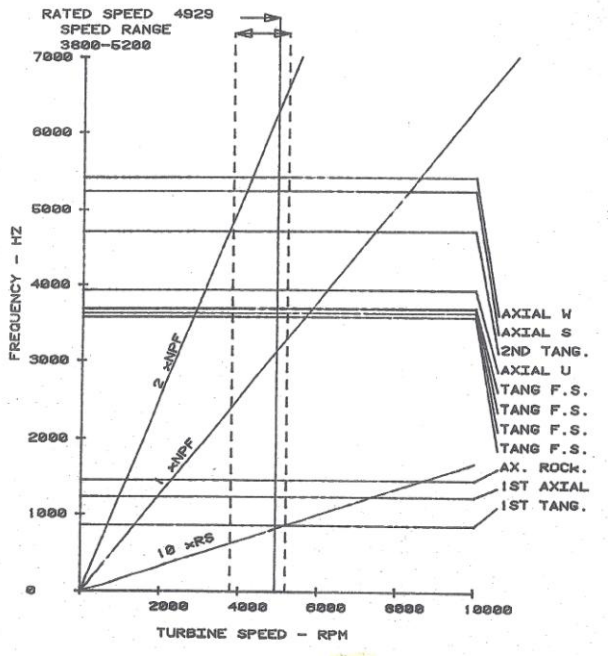


Figure 23 Campbell diagram for Modified (6 Blades/Packet)

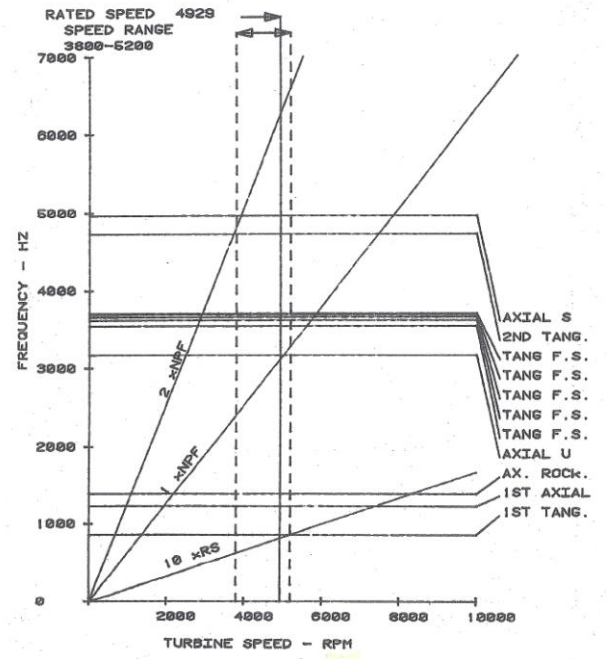


Figure 24 Campbell diagram for Modified (5 Blades/Packet)

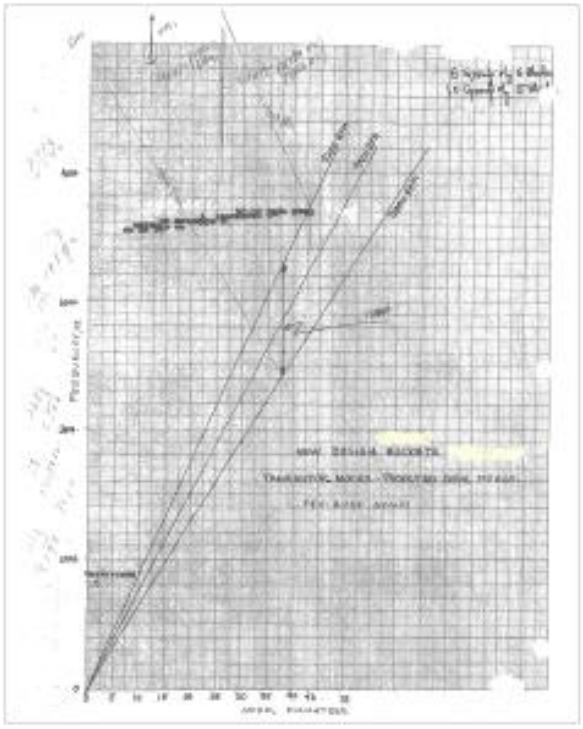

Figure 25 Safe diagram for Modified Design (Tangential Modes)

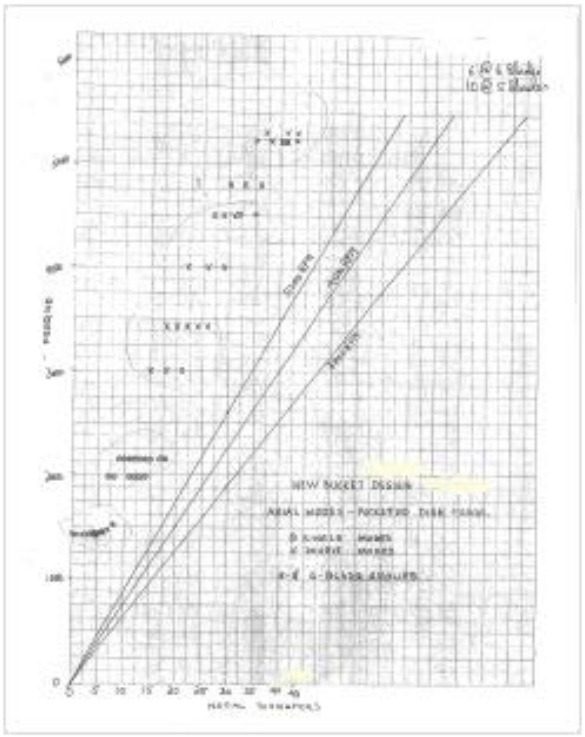

Figure 26 Safe diagram for Modified Design (Axial Modes)

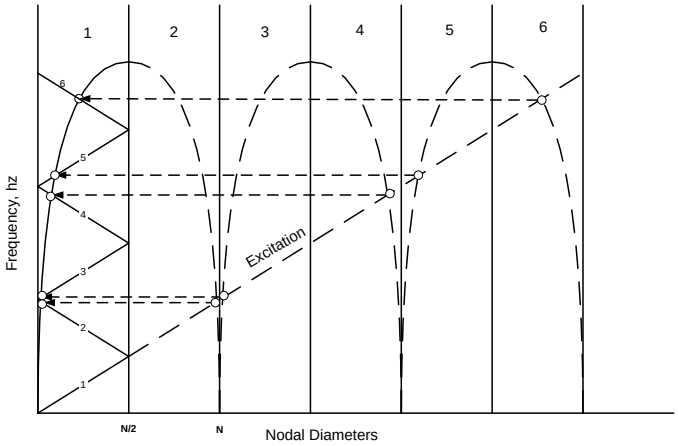


Figure 27 Wrapping of Resonance Points to half of blade count (Safe diagram)

At this time at the request of the President of Turbodyne, I presented the findings to employees. Question was raised about the excitation harmonics greater than the half of the blade count by Dick Parker of Human Resources who was in attendance. He mentioned that if the number of nozzles is greater than the half of the number of blades then there is no possibility of resonance. At this time Safe diagram did not consider reflection of excitation lines. There was no answer readily available but I knew that is not right. Looking into this matter, it became clear that it is question of wrapping the excitation lines also. Figure 27 describes that practice. Singh and Lucas (2011) describe this in detail and provide mathematical expression to determine the modes of concern.

## SAFE DIAGRAM FOR IMPELLERS

The reliability of centrifugal compressors for the most part depends on the reliable operation of impellers. Fatigue damage has been observed in blades, discs and covers. The damage is attributed to alternating stress resulting from vibration of structure. Alternating force can excite natural mode(s) of vibration that in turn may result in high alternating stresses.

Nelson (1979) stated that one possible cause of high alternating stresses is the resonant vibration of a principal mode. The vibratory mode most frequently encountered is of the plate type involving either the cover or the disc. Nelson described a fatigue failure pattern that originates at the outside diameter of the impeller adjacent to blades and fatigue crack propagates along nodal lines on the disc or the cover. Finally, a thumbnail shaped material tears out.

The modes responsible for the fatigue cracks described by Nelson are those that exhibit primarily axial motion of the disc and the cover. Another type of failure experienced in an impeller is “a thumb nail” or “scallop” shape fatigue cracks in blades. Figure 28 shows picture of such a failure in an impeller having fatigue cracks in blades. Fatigue cracks of this type in

blades are the characteristic of modes in which blade motion is predominant. Typically, motion of the structure in the modes associated with this type of failure is primarily in the tangential direction.

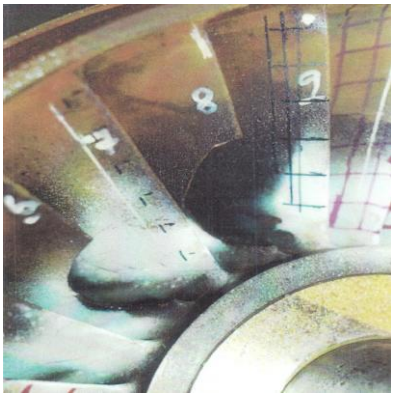

Figure 28 Photograph showing Thumb Nail or Scallop Fatigue Cracks in an Impeller

An impeller consisting of blades, disc and cover is one system. The structure vibrates as a whole. In some modes of vibration, the blades might be moving more than the cover or the disc. On the other hand, the cover might move appreciably more than the blades in some modes. The modes of vibration of a closed impeller are similar to those of a continuously banded (shrouded) bladed disc as used in steam and gas turbines. However, the interpretation of modal results can be confounded by the complex coupling between the cover and disc caused by the twisted blade of many impellers.

Analysis of a blade by itself or for that matter disc or cover by themselves is easier. However, in reality, the impeller is a system that combines the blade, disc and covers same as bladed disk for steam turbine, axial compressor or gas turbine disk. Singh etc (2003) described the behavior of each individual component as well as impeller as a system.

The impeller of a centrifugal compressor is a circular symmetric structure as a bladed disk. FE analysis was conducted for a simple (both open and closed) impeller. The impeller analyzed was a "2-D" blade design i.e. blades extend straight out from the disc to the cover. With the results of FE analysis impeller as a system was rationalized. A method to create Safe diagram based on the results of blade alone, of disc alone and finally impeller as a system was described.

The same two conditions as mentioned earlier for bladed disc were found applicable. For a state of resonance: frequency of the exciting force equals the natural frequency of vibration and the profile (shape) of the applied force should have the same shape as the mode shape associated with that natural frequency.

Mathematical expressions for natural modes and forcing function are similar to that of bladed disk as given earlier in equations 1 thru 3.

Where

K = number of distortions in flow per $360^0$, e.g. number of IGV or number of vanes, in the diffuser, etc.

N = Compressor's speed, RPM

K also represents the shape of the excitation as k nodal diameter. Equation (5) for work done is also applicable here.

*Results of Finite Element analysis*

A finite element analyses included single blade, the disc alone, an open impeller and an impeller with cover.

*Single Blade*

A single blade was modeled by using brick type elements. Two different boundary conditions were used. First, the blade was considered cantilevered with the disc. This analysis simulated single blade mode shape with the mode shape of the open impeller. For the second analysis, the nodes of the blade coincided with the nodes on the disc and the nodes on the other face of the blade coincided with the nodes on the cover. The second case simulated the blade mode shapes with the mode shapes of impeller with cover.

*Mode Shape for Single Blade*

The FE model is shown in Figure 29 with a fixed boundary condition. The nodes of the blade that coincide with the nodes on the disc surface were constrained in all directions. The first two mode shapes of vibration are shown in Figure 26. The information of interest is the displacement pattern of these modes and how it is related to the vibration pattern of blades of the open impeller.

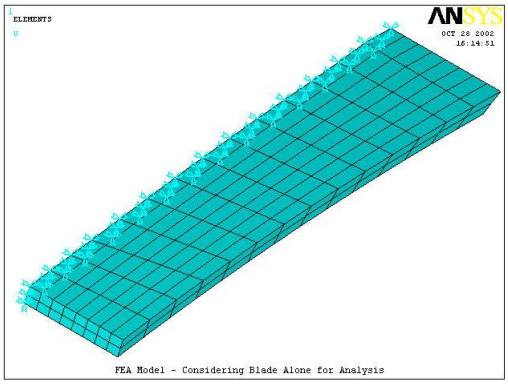


Figure 29 Finite Element Model for Single Blade

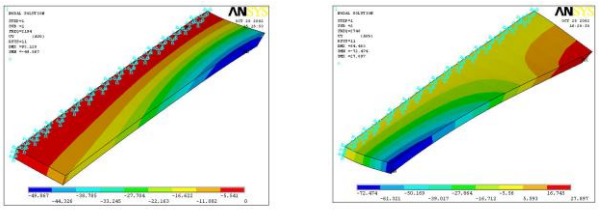

Figure 30 First Two Bending Mode Shapes of the Cantilevered Single Blade

The first two mode shapes for blades constrained at both ends are shown in Figure 31.

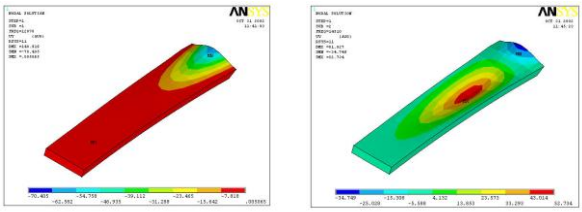

Figure 31 First Two Bending Mode Shapes of a Single Blade fixed at both ends

**DESCRIPTION FOR 3 D FEA MODEL OF IMPELLER**

The FEA model has been created using ANSYS 3D brick element (8 nodes). Each node has three degrees of freedom. These are translations in the nodal x, y and z directions. The impeller that has been analyzed has 23 blades.

*Mode Shape of Disc Alone*

The finite element model of the disc is given in Figure 32. Few mode shapes are also shown from Figure 33 and Figure 34.

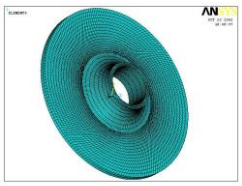

Figure 32 Finite Element Model for Disc Alone

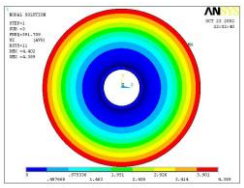

Figure 33 Umbrella (0 Circle and 0 Nodal Diameter Mode) for the Disc

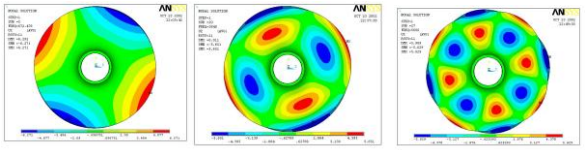

Figure 34 Representative Mode Shapes for the Disc

*Mode Shapes of Open Impeller*

An analysis was performed for an open impeller that contained the disc and 23 blades previously analyzed. The FE model is shown in Figure 35. A few mode shapes are also shown in Figure 36 and Figure 37.

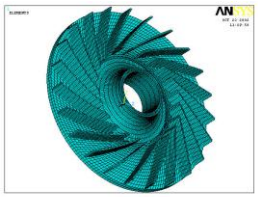

Figure 35 Finite Element Model of Open Impeller

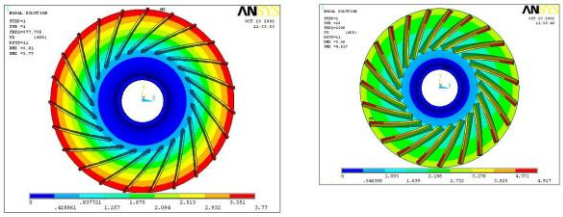

Figure 36 Umbrella (0 Circles and 0 Nodal Diameters) Mode Shape of the Open Impeller, Displacement in the Axial Direction and in the Tangential Direction

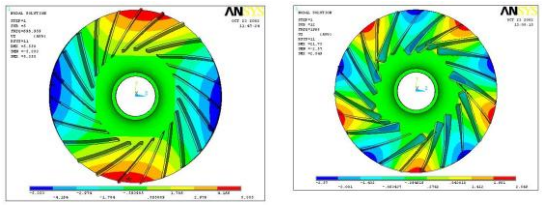

Figure 37 0 Circles and Few Nodal Diameters Mode Shapes of the Open Impeller

*Mode Shape of Impeller with Cover*

An analysis was also performed for an impeller with a cover that has the same 23 blades described earlier. An FE model is shown in Figure 38. Mode shapes are also shown in Figure 39 and Figure 40.

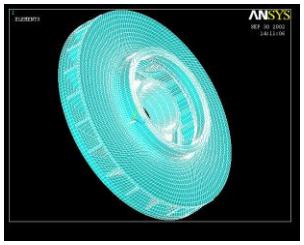

Figure 38 Finite Element Model of Impeller with Cover

Figure 39 Umbrella (0 Circles and 0 Nodal Diameters) Mode Shape of the Impeller with Cover

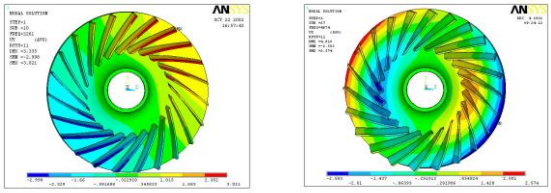

Figure 40 0 Circles and 1 Nodal Diameter (Tangential Displacement) and 1 Circle and 1 Nodal Diameter Mode Shape (Axial Displacement) of the Impeller with Cover,

## POSSIBLE FORCING FUNCTION FOR IMPELLER

Singh and Lucas (2011) described some possible forcing for centrifugal compressors. The most obvious sources of excitation are 1x or higher order interactions with the number of diffuser vanes, inlet guide vanes (IGV), return channel vanes (upstream or downstream of the impeller) and impeller blades. For single stage units such as pipeline compressors, a volute tongue is a possible excitation source. Volutes (and to a greater extent collectors) create non-uniform pressure fields at the discharge of the impeller that could act as a forcing function. Stall is also a potential source of excitation and can occur within the impeller or the diffuser (with vane or without vane). Stall in diffusers without vanes is characterized by one or more "cells" that rotate with (although slower than) the impeller. Stall cells have been known to cause high sub-synchronous vibration. The disc/cover cavity shape (the shape of the cavity between the disc or cover and the stationary walls surrounding the impeller) has also caused acoustic resonance that resulted in impeller failure.

Safe diagram is found to be an excellent guide in determining the possibility of exciting a particular mode of vibration in an impeller. The x-axis of the diagram represents nodal diameters. Frequency is plotted on the y-axis of the Safe diagram. A good design would yield a Safe diagram that indicates no coincidence of possible excitation force with a natural mode of the impeller (tuned system). Results of the modal analysis have been used to draw a Safe diagram.

Displacement pattern of mode shapes around the disc and cover were decomposed thru Fourier analysis. It was found that many harmonics were present in mode shapes but there was a predominant harmonic. For plotting Safe diagram the largest component of harmonic is used to name that mode. Plots of mode shapes were also used to verify the Fourier results and to determine the number of circles present in these modes.

Results of the Fourier analyses were divided into axial and tangential directions. If the amplitude of displacement is in axial direction then it is termed as axial mode and it is termed tangential if displacement is in the tangential direction. Mode shapes in the first family consisted of each blade displaying the first bending mode of a single blade, see Figure 41.

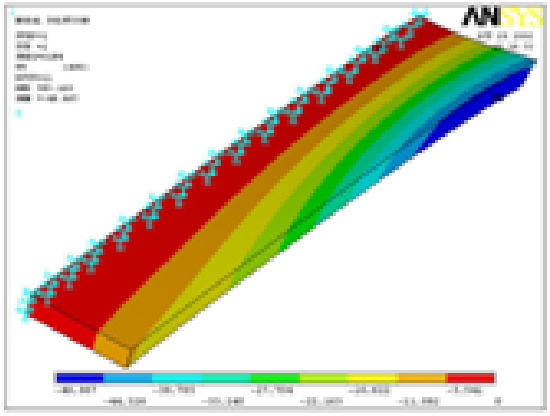

Figure 41 Modes where the Blade shows the first mode of a cantilevered blade

Each mode shape consists of a different number of blades moving in the same or opposite direction. For example, if half the number of blades moves in one direction, and the next half move in the opposite direction, there is one phase change in the displacement. The pattern of displacement is similar to a single cosine or a single sine wave. Thus, it is called one nodal diameter.

Utilizing the concepts and methods discussed in earlier sections the finite element analyses results for the cases studied in the form of Safe diagram have been plotted in Figure 42 and Figure 43.

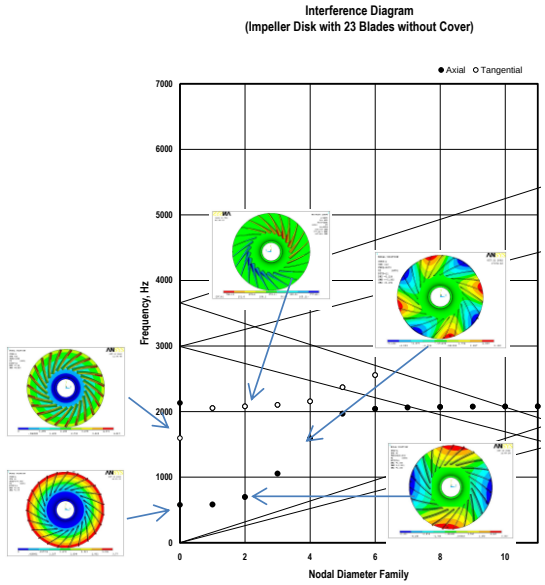


Figure 42 Safe diagram for Open Impeller

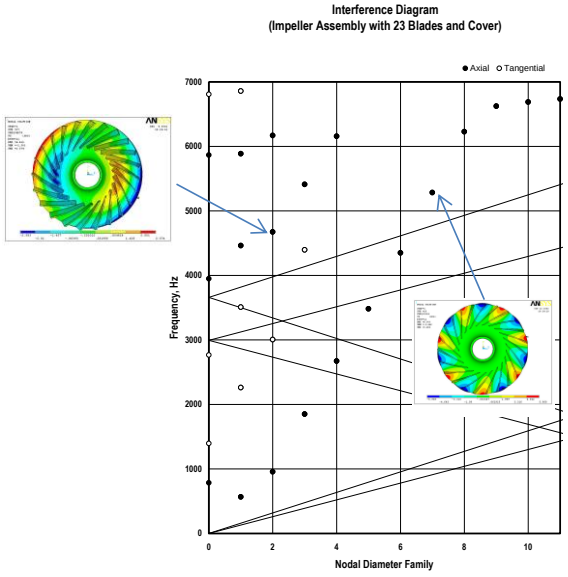


Figure 43 Safe diagram for Closed Impeller

## SAFE DIAGRAM FOR MISTUNED SYSTEM

Including geometrical variations among blades was the next logical advancement in the analysis of the dynamic response of blades. It has been shown that geometrical variations influences mode shapes and frequencies and in turn, the response of a bladed disk system. In a tuned system where each blade is identical, modes in general occur in duplicate. There are two modes that differ by a phase angle but these modes have identical frequencies. However, when symmetry is disturbed through variation from blade to blade, these modes tend to split in two frequencies. Also, the shape of these modes get distorted from the tuned case, which is a phenomenon called "mistuning". Ewins (1976) has extensive discussions of this phenomenon and the response of the mistuned case was found to be different from the tuned case. This was attributed mainly due to a change in the mode shape and may pose a serious decision point for designers to account for variability among blades. Ewins specifically dealt with completely shrouded or un-shrouded bladed disk constructions.

Irregularity in the bladed disk system makes the response of the system asymmetric. These irregularities can be caused by structural and/or aerodynamic means. Structural irregularities arise due to variations in geometrical dimensions from blade to blade; it can also be complicated due to variations in the boundary conditions and due to variations in the fixity of blades to the disk or cover. Frequencies may be different than in the tuned case and the mode shapes are non-sinusoidal. Irregularities in the aerodynamic forces come from variation between guide vanes opening. This causes force around the periphery of the disk to be of a non-sinusoidal form. Mode shapes and forces though non-sinusoidal are periodic in nature. Fourier decomposition of these with respect to the angular position around the disk will yield harmonics in addition to that of the tuned case, which results in a different response of the blade compared to the tuned case.

For a tuned system, frequencies occur in duplicate, i.e., there are two identical frequencies for a given mode shape. These shapes are graphically the same, but differ from each other by a phase angle. Structural mistuning results in a phenomenon called "splitting of frequency". Splitting separates these frequencies for each mode and the amount of separation of frequencies depends on the amount of mistuning. For example, a three nodal diameter pattern of a disk might occur at two frequencies. In general, these frequencies crowd the Campbell diagram and the Safe diagram yields a clear depiction of this phenomenon.

The analysis of a mistuned bladed disk system becomes complex. Due to manufacturing variations, blades on the same disk will be different from each other even when they are within manufacturing tolerances. Their contact condition in the disk slot may also be different. Therefore, assembly of these blades on a disk will be random unless each blade is individually measured and its location on the disk noted. Sometimes the location is chosen in order to balance a disk containing long blades. However, even known locations pose difficulty in analysis. Each bladed disk produced in such a manner from the same lot of blades will be different and therefore, their vibration characteristics will also be different. The complexity of the analysis is compounded by the presence of a large number of blades on the disk.

Ewins (1969) reported that for a given excitation and damping conditions, the response in one mode (or pair of modes) depends on the amount of "split" of the two natural frequencies. The presence of slight mistuning, small blade imperfections, can cause resonant stress levels in some blades

up to 20% higher than equivalent tuned case. This kind of increase depends on the specific arrangement of the blades around the disk. He also noted that by careful arrangement of the same set of non-identical blades, it is possible to eliminate the risk of such an increase in the peak stress level. Ewins (1976) reported the results of a study of a slightly mistuned bladed disk. The study considered a group of nominally identical blades. Various dimensional variations in blades nominally result in about $\pm$ 2 to 3 % variation in a 1F frequency. Even though there is a slight change in frequency the result showed that the effect on mode shapes is large. This phenomenon of variation in the mode shape has considerable effect on the response of the blade. The main interest in the design of a blade is its response under load; hence mode shape should be critically examined. Singh and Ewins (1988) and Singh (1992) presented probabilistic analysis results by considering a random arrangement of blades on the disk utilizing Monte Carlo simulation.

The analysis reported earlier for the packeted bladed disk may be considered as deliberate mistuning. This was attributed to the breaking of a continuous shroud band into packets at some predetermined locations. This permits some modes to be split and it has been used successfully in packeted bladed disk design.

For a mistuned bladed disk system, the vibration energy is unevenly distributed among all blades of the disk. The mode shapes may be far from a regular sinusoidal shape. The examination of modes in such a situation is done using Fourier decomposition of the displacement pattern to obtain harmonic contents. On a Safe diagram, the mode is named in accordance with the largest content of the harmonics of the Fourier decomposition of the mode shapes.

Following discussion of mistuning is applicable to any circular symmetrical system (e.g. bladed disk, impellers etc.) in case of a geometrical mistuning or force mistuning or both.

*Safe diagram for perfectly tuned case-structural and forcing*

As explained earlier for this kind of system, each mode occurs in pairs with equal frequency. One exception is that 0 ND mode is always single. Depending on the blade count the last mode may also be single. For discussion sake a Safe diagram for such a system having 48 blades is shown in Figure 44. Each circle represents double modes except the 0ND mode and 24 ND modes.

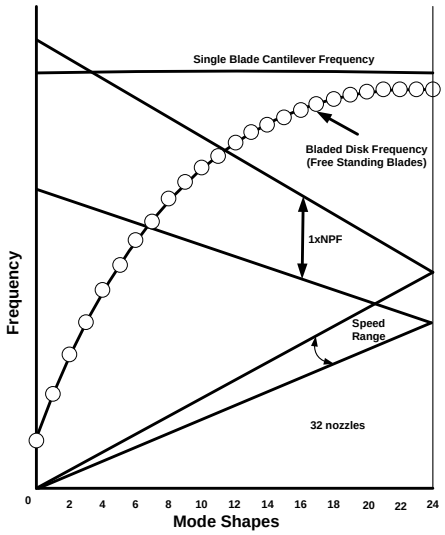


Figure 44 Safe diagram for Tuned System (courtesy: Safe Technical Solutions)

**SPLITTING OF MODES IN TWO FREQUENCIES**

In the case of random mistuning it is expected that frequency of each mode will split in two frequencies and both modes become distorted i.e. these are not symmetrical as shown in Figure 45. The amount of separation between two resulting frequencies will depend on amount of mistuning. The resulting response curve is the summation of the response of these modes separately.

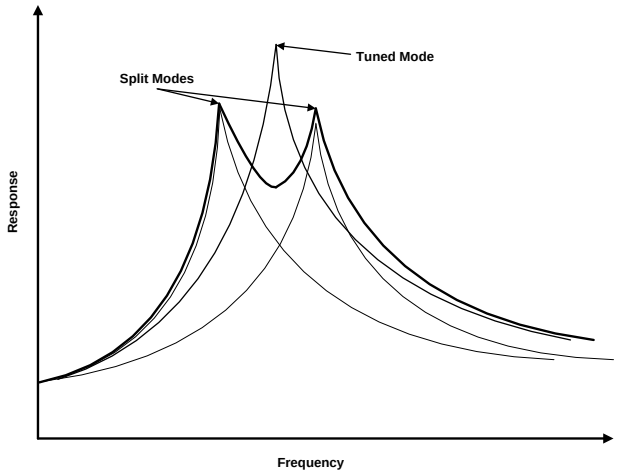


Figure 45 Split Frequencies due to Mistuning (Courtesy: Safe Technical Solutions)

It has been practice to display these separate frequencies on the Safe diagram to assess the effect of this phenomenon. Figure 46 shows such a feature just for two modes for demonstration purposes. It is expected that for random structural mistuning nearly all modes may split. Examination of this figure shows that response due to excitation will occur at the mistuned frequencies.

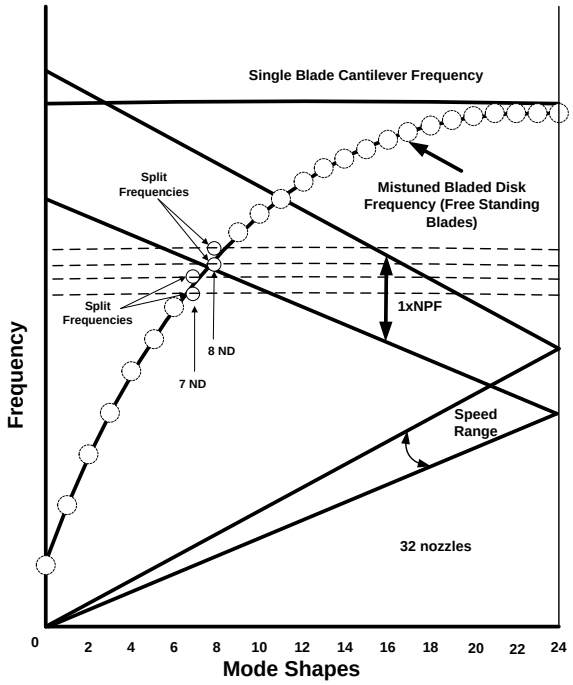


Figure 46 Split Modes Plotted on Safe diagram (Shown for just two modes for explanation) (Courtesy: Safe Technical Solutions)

## RANDOM MISTUNING (STRUCTURAL)

When the frequencies split, other effect is that the modes become distorted. These modes display many harmonics which otherwise contained only one harmonic for the tuned case. Figure 47 thru Figure 49 depict harmonic contents of these distorted modes.

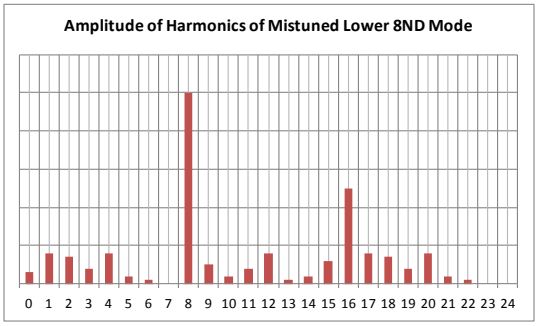


Figure 47 Harmonic Contents for Lower 8ND Mode due to Mistuning (courtesy: Safe Technical Solutions)

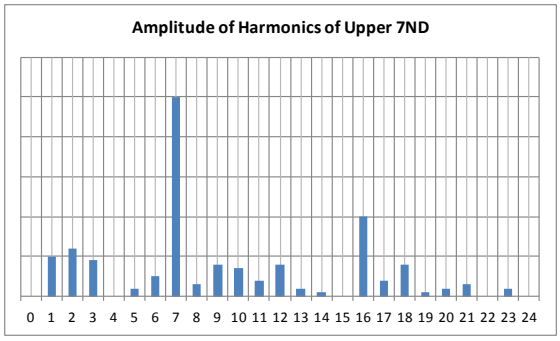


Figure 48 Harmonic Contents for Upper 7ND Mode due to Mistuning (courtesy: Safe Technical Solutions)

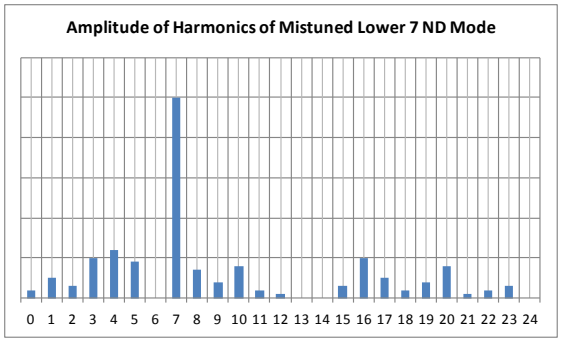


Figure 49 Harmonic Contents for Lower 7ND Mode due to Mistuning (courtesy: Safe Technical Solutions)

## SAFE DIAGRAM FOR STRUCTURAL MISTUNING WITH TUNED FORCE

Examination of Safe diagram (Figure 46) points towards close attention to the distorted modes as shown in Figure 47 thru Figure 49. Figure 50 shows the way this phenomenon has been considered using Safe diagram. This shows the consideration of 1xNPF excitation and upper 7ND mode. Even though the concept of pure resonance (for tuned system) 7ND mode is not considered, it is evident that there are 16 harmonics in this mode. This portion of the harmonic of the mode shape will be excited by 1xNPF (16 harmonic of force). Consideration for the split 8 ND mode is taken care of same way. Equation developed earlier for work done shows that there will be response but it will be forced response.

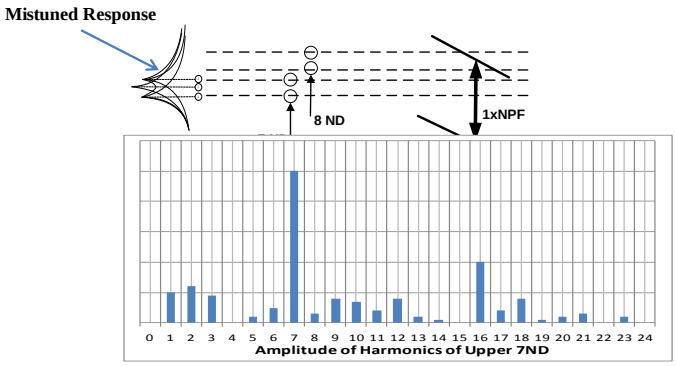


Figure 50 Representation of Split Mode and Contribution of Harmonic Content for Upper 7ND Mode for Structural Mistuning (courtesy: Safe Technical Solutions)

## FORCING DISTORTION

Unsteady forces due to effects from the rotating blades passing the stationary nozzle partitions are possibly the most important, and consequently the most studied, source of excitation for blade vibration in axial flow turbines. These forces arise mainly because the nozzle vanes' or partitions' trailing edges have finite thickness, and because the gas is discharged toward the moving blades via discrete nozzle passages which are subject to a variety of small variations in geometry (Fig. 51). In turn, these produce a variety of flow non-uniformities and disturbances at the nozzle exit, immediately upstream from the moving blade row.

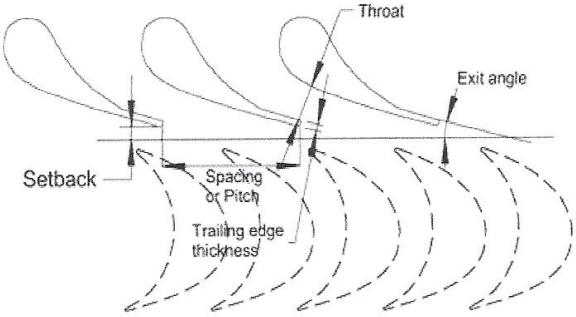


Figure 51 Nozzle Geometry Definitions

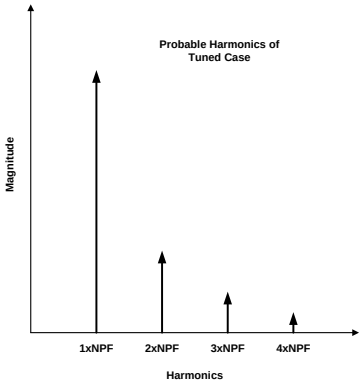


Figure 52 Multiple NPF Content for Tuned Nozzles

If the nozzle assemblies were perfect, with each partition perfectly placed so there are no variations in nozzle exit area, nozzle spacing, and setback distance, the designer would have to consider only the fundamental nozzle passing frequency (i.e. 1X nozzle passing) and its low multiples (2X, 3X, and so on) – pure tones in other words - when analyzing the frequency response of the rotating blades (Fig. 52). However, since these nozzle characteristics always exhibit variations as a result of manufacturing tolerances (refer to Figure 53), variations in nozzle exit area, circumferential pitch or spacing, and setback in otherwise pure signal at 1X nozzle passing frequency, and superimpose other harmonic frequencies on the predominant 1X nozzle passing frequency "signal" or forcing function (Fig. 54). Although this is primarily concerned with variations from design values due to manufacturing tolerances, the inevitable variations that originate from erosion, wear, and foreign object damage during turbine operation can also produce potentially destructive unsteady forces on the rotating blades

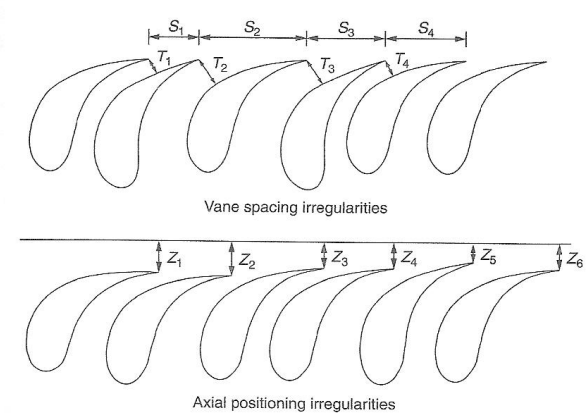


Figure 53 Nozzle Manufacturing Variations

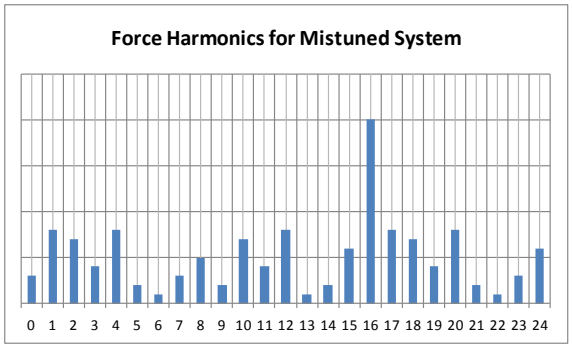


Figure 54 Harmonic Stimuli from Vane Spacing Irregularities
(Courtesy: Safe Technical Solutions)

## SAFE DIAGRAM FOR TUNED SYSTEM WITH FORCE MISTUNING

Many instances occur in design where system is almost completely tuned but the force excitation is not. Safe diagram for such a system for the modes of interest is drawn and it is shown in Figure 55. Again it shows that natural frequency matches with the frequency of excitation but due to mistuning of force only the harmonic contents of the force that match with the harmonic of the mode will contribute to the response of the system. Equation developed earlier for work done shows that there will be response but it will not be due to $16^{th}$ harmonic of the force but due to 7th and $8^{th}$ harmonics. Many times the forces are mistuned deliberately to take advantage of this phenomenon.

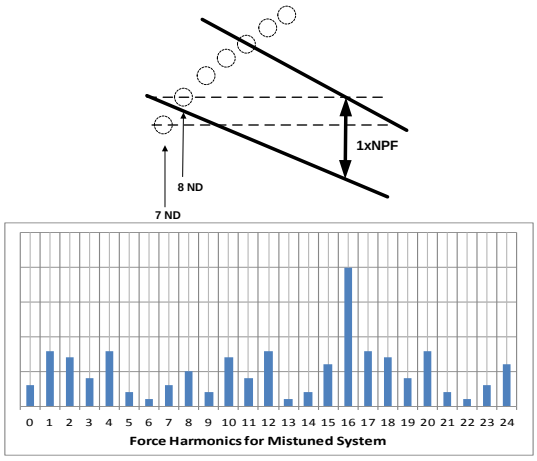


Figure 55 Safe diagram Representation of Harmonic Contents of 1xNPF Excitation for Mistuned Forcing (courtesy: Safe Technical Solutions)

## SAFE DIAGRAM FOR BOTH STRUCTURAL AND FORCE MISTUNING

Safe diagram has also been used in the general case of both types of mistuning: structural as well as forcing. Figure 56 is the Safe diagram for this situation. This is drawn again only for the modes of interest. It shows that there might be match of similar harmonics of mode shape and force and these must be known or estimated. Previously developed equations have been used to understand this phenomenon. Again this shows that it is not a case of pure resonance but forced response. Finally, response must be estimated by a forced response analysis by more accurate technique such as FEA and this should be used to determine the reliability of the design.

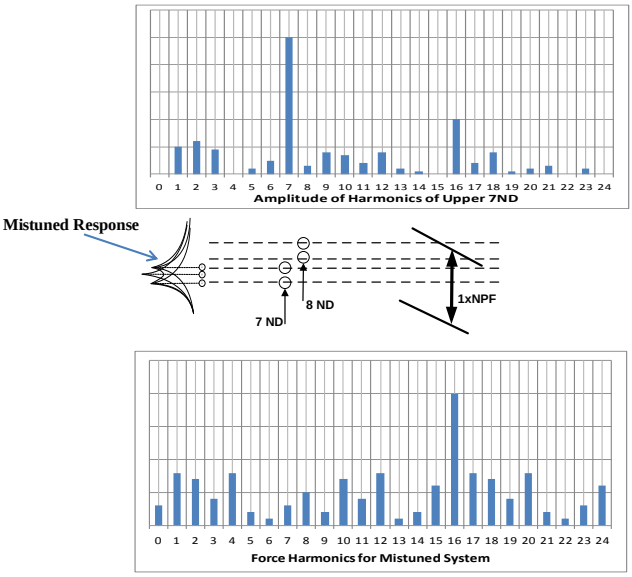


Figure 56 Safe diagram Representation of Harmonic Contents of 1xNPF Excitation for Mistuned Forcing and Harmonic Content for Upper 7ND Mode (courtesy: Safe Technical Solutions)

## INCLUSION OF CENTRIFUGAL STIFFENING IN SAFE DIAGRAM

Most of the time modal analysis is conducted without regard to the speed of the machine. Natural frequencies for relatively long blades are affected by the speed. Most of the time it is larger than that estimated at zero speed. This is called "centrifugal stiffening". For shorter blades this influence is minimal. Safe diagram for such a case is shown in figure 57 for a constant speed machine. It shows that a mode which might have been deemed benign based on estimation of natural frequency at zero speed might not be so due to centrifugal stiffening. It is prudent to conduct modal analysis including centrifugal stiffening for constant speed machine. However, it is not practical do so for a variable speed machine such as mechanical drive turbines. In this situation Safe diagram is first

drawn based on the natural frequencies at zero speed then based on the mode of interest after examining the Safe diagram, natural frequencies are estimated at the speed of concern. Designers based on experience have developed simple formula to estimate the change in frequencies without detailed analysis.

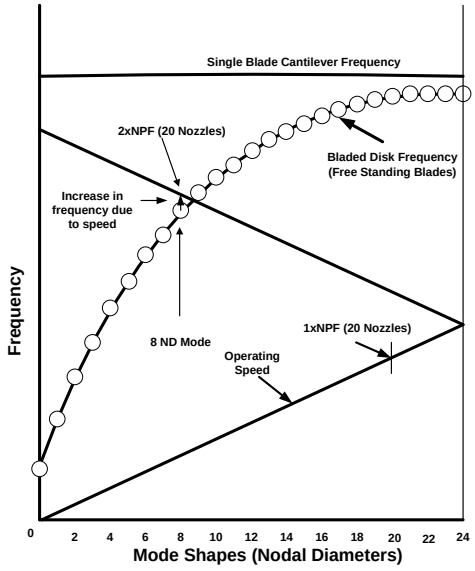


Figure 57 Safe diagram Representation to Include Effect of Centrifugal Stiffening (courtesy: Safe Technical Solutions)

## EXAMPLES OF APPLICATION OF SAFE DIAGRAMS

*An Impeller Failure*

Concept of the Safe diagram has helped in the design of reliable impellers. Also, it has helped to understand fatigue failures and thus help to formulate a solution to those failures. An impeller of a pipeline compressor showed fatigue damage in many blades after a small operation time, Figure 58 and Figure 59.

Figure 58 Scallop Shaped Break out from Blades.


Figure 59 Photograph showing Separated Scalloped Material

The shape of the separated pieces was of a “scallop” type. Based on a finite element analysis supported by a frequency test, a new impeller was designed. The solution was an impeller with modified blade geometry and a change in the number of blades of the impeller. The modified design is operating successfully in the field.

The same impeller was analyzed to create Safe diagram for the original design as well as the modified design to take a fresh look in the possible cause of damage and the remedy thereof. Finite element analysis has been performed on the damaged impeller geometry. A parallel analysis has also been performed on the modified impeller. Figure 60 and Figure 61 show the Safe diagrams for the original and for the modified impeller geometry. Figure 60 shows resonance with the second harmonic of the possible excitation force generated by IGV.

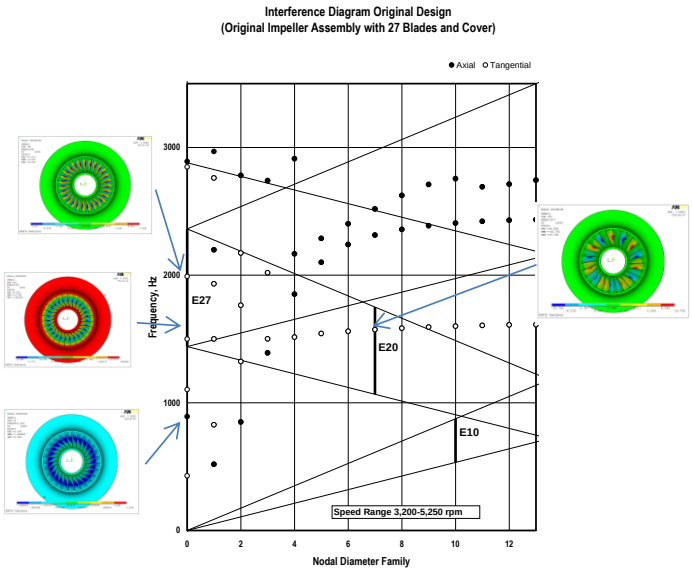


Figure 60 Interference diagram for Original Impeller

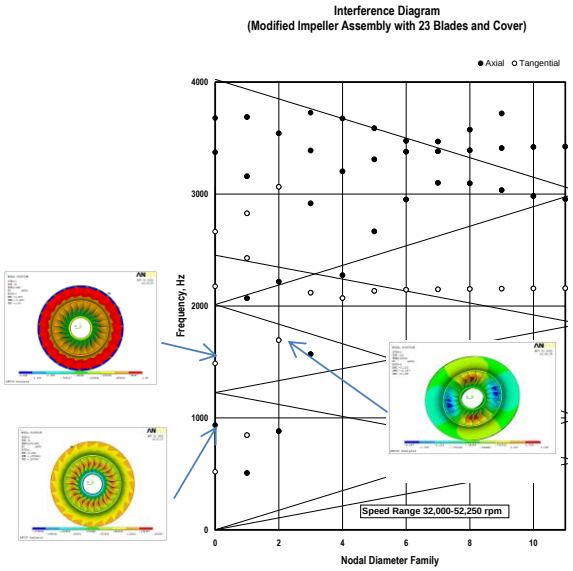


Figure 61 Interference diagram for Modified Impeller

The mode that coincides with the second harmonic of the IGV excitation is shown in Figure 62. It is instructive to note that the displacement pattern of each blade is similar to the scallop shape at the inlet where the damage occurred in the blades.

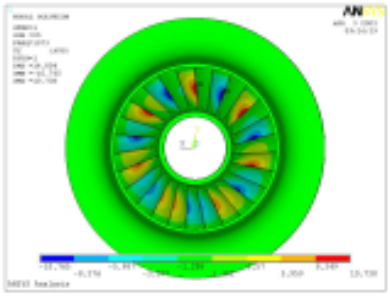

Figure 62 7 Nodal Diameters Mode with Scallop shaped Displacement Pattern for Blades.

Safe diagram also shows a possible resonant condition with a force having a shape of blade passing frequency. The force having nodal diameters equal to the number of blades can also excites a zero nodal diameter mode of vibration of the impeller if frequencies are coincident per Equation (5). There are two modes that are coincident with the blade passing excitation within the speed range, shown in Figure 63. In both modes of vibration the displacement pattern of each blade is also similar to the scallop shape at the inlet where the damage occurred in the blades.

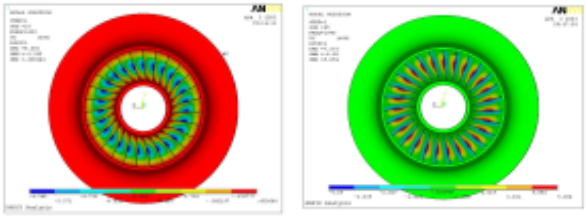

Figure 63 Zero Nodal Diameter Modes with Scallop Shaped Displacement Pattern for Blades

For a relatively dense medium and also for a high- speed application, there is a probability of a reflection of a force emanating from the rotation of blades. The impeller was modified with this in mind. The modified impeller has a different number of blades with an increased thickness. This resulted in a higher frequency for modes controlled by blades. The modified design did not have any IGV so the excitation due to vanes does not exist. The Safe diagram (Figure 61) of this design also shows the possibility of blade passing frequency exciting a mode of zero nodal diameters.

The original impeller failed very quickly indicating a high cycle. Fatigue mode of failure but the redesigned impeller has been in operation for a long time without any distress. It can be inferred from this study that second harmonics of the vane excitation might have been responsible for the damage of the original impeller. Figure 61 shows that if the reflected blade passing force was the cause of failure, then the modified design should have shown damage in operation.

Safe diagram is successfully used to explain the failure and for modification of the impeller when there is scalloped shaped failures in blades. It can be similarly applied to scalloped shaped failures in a cover and / or disc. The failure in blades is attributed to tangential modes since blades vibrate primarily in tangential direction. The scalloped shaped cover and disc failures are be attributed to axial modes in which the primary displacement is in the direction of the axis of the machine.

*Radial Inflow Turbine Disc*

A radial inflow turbine's impeller had a history of several early failures in the highly erosive, brine steam environment attributed to stress corrosion cracking (Singh etc, 2007). Several mitigation actions were taken in impeller material and process cleaning equipment. Impeller had a coating of a thin layer of tungsten carbide to protect the wheel against erosion due to minute solid particles in the steam. A crack was discovered during a routine inspection of the turbo-expander wheel after a successful operation for nine months. This crack was located at the coating surface at the base of one blade by using fluorescent penetrant inspection (FPI) during a maintenance outage. The coating was mechanically removed to inspect the entire wheel for cracks in the substrate. No crack

was detected through FPI examination anywhere in the wheel after removal of the coating. Wheel was laser shock peened for better fatigue resistance in the fillet area near the base of each blade. Laser shock peen was done to provide localized compressive stress in the fillet radii areas. This wheel was then put in service uncoated.

After a few hours of operation wheel airfoil was reported to have fractured. Examination of the wheel revealed that the initiation site of final fracture was at the base of a blade. It was also established that it was the same blade at the same location in which the coating was found cracked earlier (Figure 64).

Figure 64 Crack Locations in the Coating and the Final Separation Site.

It was noted that a large area of the fractured surface was discolored indicating oxidation of the surface. This might indicate a pre existing crack. This fact indicated that either the inspection technique to find crack was not capable of picking a tight crack or the coating removal process might have masked the existing crack.

It was suspected that the erosive/corrosive nature of geo-thermal steam was contributing to the initiation of the crack in the coating and then the existing stresses though small might be responsible of propagating it to fracture. The quality of steam was good since new process scrubber equipment was added and the steam did not have many erosive/corrosive species reported in sampling. The spare wheel was put in service that was identical to the damaged one. The main reason for this was the suspicion that environment was initiating crack in the coating. Hence, initiation of crack was not envisioned.

Detailed analyses were initiated to examine the possibilities of failure due to resonance with excitations resulting from harmonics of inlet guide vanes (IGV) (up to fourth harmonics were considered), to examine failure due to other modes during start up below the operating speed and to explain the initial cracking in the coating,

The analyses included the following:

a) Finite element steady state stress analysis under centrifugal loading.
b) Modal analysis to include or exclude the possibility of resonance. Concept of Safe Diagram for Impellers was used for resonance identification
c) Harmonic forced response analysis was performed to estimate dynamic stresses. Harmonic response analysis had been conducted for the modes of interest as inferred from the Safe diagram.
d) Classical fatigue analysis was conducted to understand the possibility of initiation of crack near the base of the blade.

Finally, corrective action(s) are defined based on the knowledge gained from the analyses.

*Description of analysis and results*

Steady state stress resulting from centrifugal loading has been estimated using finite element method. A sector of the wheel containing one blade was modeled (Figure 65). It is efficient to use one wheel sector containing one blade and the boundary condition is represented by cyclic symmetry.

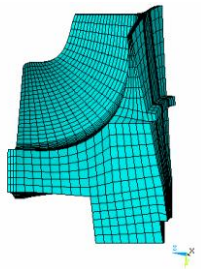

Figure 65 FE model for Steady State Analysis

Contour plots of the resulting stress are shown in Figure 66.

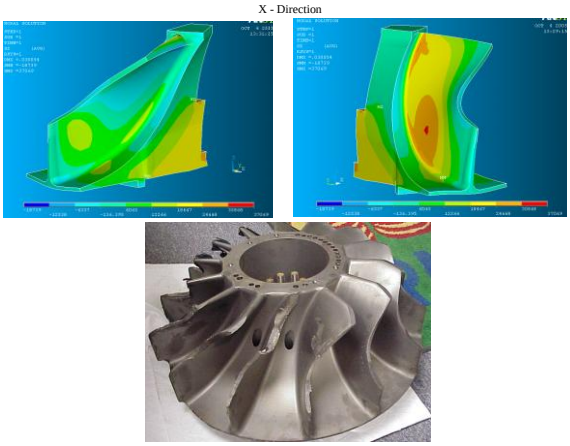


Figure 66 Contour of Radial Stress at 12400 rpm

*Modal Analysis*

A new FE model was created for the modal analysis. It contained the complete wheel with 14 blades and the disc (Figure 67). It was anticipated that harmonic response analysis will be performed and for that a complete model was required. The nodes at the bolt circle have been constrained for all degrees of freedom.

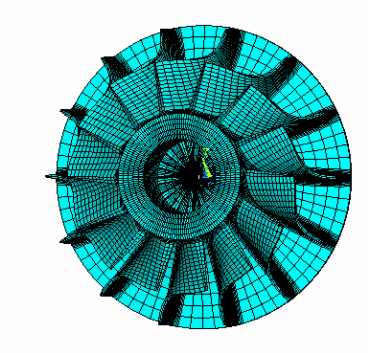

Figure 67 Model of the Wheel for Modal Analysis

Some representative mode shapes are plotted in Figure 68. It should be noted that the first mode is a 1 ND and the second mode is a 3 ND.

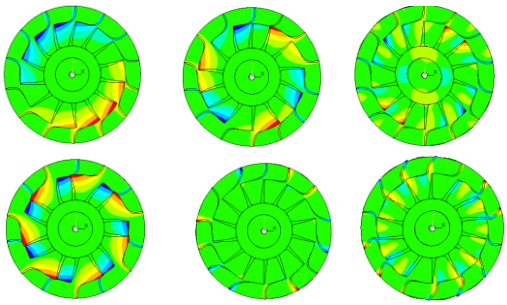

Figure 68 Some Representative Mode Shapes

Due to axi-symmetric geometrical shape of the wheel, modes occur in duplicate. These modes have identical frequencies. Nodal diameters of the duplicate modes occur at a different angular position even though these have same number of nodal diameters. Frequency of each mode is plotted against its shape on the Safe diagram. It is shown in Figure 69. The radial line represents the operating speed of 12400 rpm.

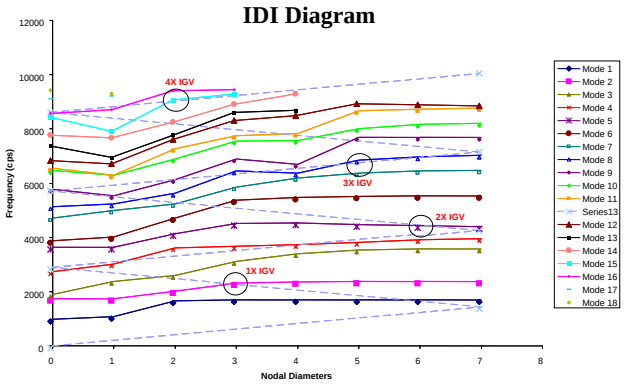


Figure 69 Safe diagram for the Wheel at 12400 rpm

The modes of interest have been identified on the basis of the possibility of exciting the wheel by the forces generated by IGV. Excitations up to 4th harmonics of IGV have been considered.

*Harmonic Forced Response Analysis at the operating speed of 12400 rpm.*

For the first harmonics of excitation the force is applied to the mode shape as shown in Figure 70 with blade arbitrarily numbered. Figure 68 show the magnitude of load distribution for each blade for the first harmonics of IGV excitation.

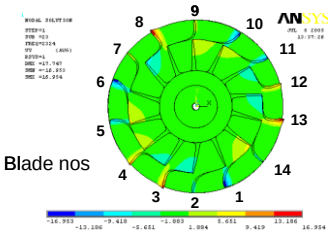


Figure 70 Blade Numbering

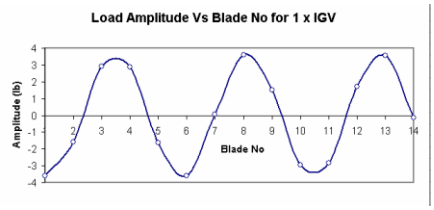


Figure 71 Distribution of Load on Blades for 1xIGV

Similarly, force distribution for the second, third and fourth harmonics also had been developed for harmonic forced response analysis. The damping ratio used in the calculation was 0.0008. This is almost equal to material damping and it had been used to estimate the worst response level. Figure 72 shows the amplitude of vibration as a function of exciting frequencies at different locations on the blade.

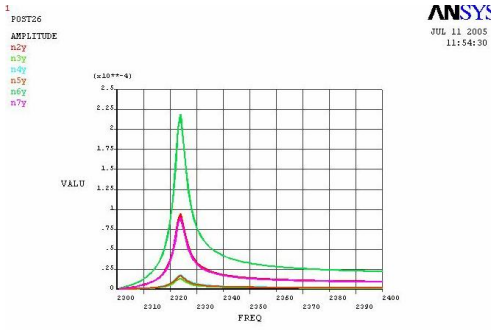


Figure 72 Displacement Responses vs. Frequency of Excitation

Figure 73 has the exploded view of the area of high stress. It should be noted that these peak stresses do not occur at the location of the initiation of cracks.

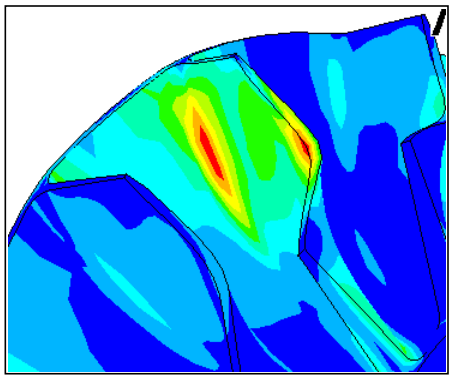

Figure 73 Detailed Views

*Harmonic Forced Response Analysis for 3 ND mode (1694 Hz) that may be excited by 1xIGV harmonics at 9240 rpm.*

The estimated stresses due to the excitation forces of harmonics of IGV at 12400 rpm are not considered to be large enough to do fatigue damage. The estimated factor of safety is large. Moreover, the location of peak stress is not near the crack initiation site. There is another three nodal diameter mode at an estimated frequency of 1694 Hz. However, this mode may be excited by 1xIGV excitation during start up of the machine at an estimated speed of 9240 rpm. Harmonic forced response analysis was performed for this mode at 9240 rpm.

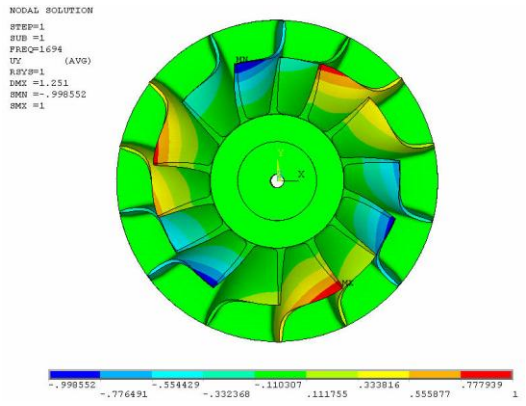


Figure 74 The 3 ND Mode Shape at 1694 Hz

Figure 74 shows the 3 ND mode shape that is being considered for further harmonic forced response analysis. Distribution of forces per blade and the relative magnitude of the force on each blade were the same as used in the earlier response analysis.

Amplitude of vibration as function of exciting frequency is given in Figure 75.

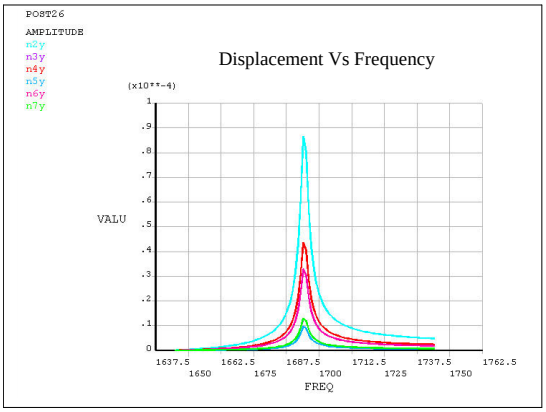


Figure 75 Vibration Amplitude as a Function of Excitation Frequency

Figure 76 show the picture of the failed wheel side by side the contour plot of stress resulting due to excitation of the mode (3 ND) at about 1694 Hz by 1xIGV. It is very informative to note about the coincidence of the location of crack initiation site and the peak stress.

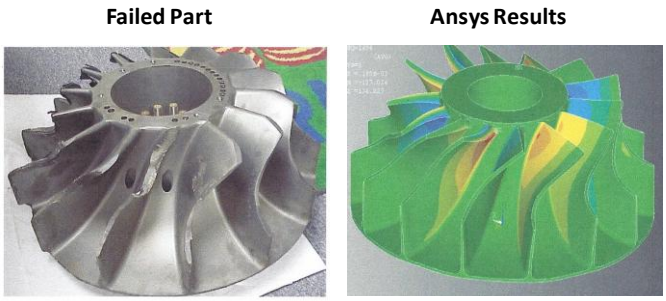


Figure 76 Picture of Failed Wheel and Stress Contour Plot

*Summary*

a. Safe diagram indicated four modes of interest from resonance point of view at the running speed of 12400 rpm. These modes were near 1xIGV, 2xIGV, 3xIGV and 4xIGV excitation frequencies respectively.
b. The location of maximum stress is not at the damage initiation location. Hence, a pure resonance up to 4$^{th}$ harmonic of IGV excitation is not likely for the observed initiation of crack in the wheel without coating. At design speed, interference due to multiple of expander IGV wake counts was ruled out as possible cause of wheel failure. Pattern of stress was inconsistent with the failure mode of the blade.
c. Another 3 ND mode exists at about 1734 Hz after the calculated frequency was adjusted for the effect of temperature (calculated frequency is 1694 Hz). This mode may be excited by 1xIGV at about 9458 RPM. Furthermore, the location of peak stress coincides with the location of crack initiation site on the wheel.

d. Final separation of blade of wheel was due to pre-existing cracks in one of the root of the blade.
e. Initially, the crack initiated in the coating due to low fatigue property possibly due to frequency interference of synchronous frequency with a 3 nodal diameter mode during start up. For uncoated wheel, magnitude of stress was low enough to initiate a crack in the parent material. However, when a crack was initiated in the coating, magnitude of stress was sufficient to grow this crack to final separation.
f. The startup procedure was modified to avoid damaging fatigue cycles and to reduce the effect of possible excitation frequencies during every start up at 9240 rpm.
g. Based on the frequency response analysis results and conclusions, it is concluded to be safe to continue using the spare wheel under the existing clean steam condition. Wheel that is currently in use should be replaced with the available new wheel with partially removed coating.

## IMPURE MODE SHAPES (PACKETED BLADED DISK)

The continuous shrouded bladed disk and bladed disk without shroud are tuned systems if each blade has the same form and dimension having the same fixity in the disk. Due to the dimensional variations from blade to blade, these identical frequencies for a mode split into two frequencies for the same mode. The shape of the mode may contain other than primary harmonics. This phenomenon is commonly observed in a packeted disk assembly. This is a case of deliberate mistuning, i.e., mistuning is introduced by breaking shroud at specified interval. This breaks the geometrical symmetry of the bladed disk. An example is presented to demonstrate the implication of irregularities in the mode shape due to packeting and asymmetry of the aerodynamic forces. Singh and Lucas (2011) described a case. Assumption is made that each blade is identical so that no mistuning is introduced due to a variation in the blades.

A finite element model of a bladed disk with 60 blades (10 packets with 6 blades in each packet) is shown in Fig. 77.

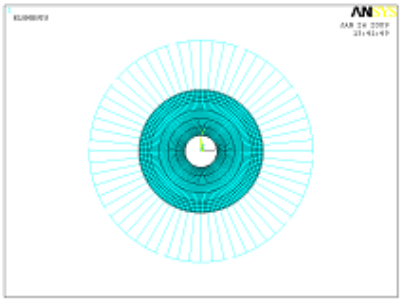

Figure 77 Model of a Packeted Bladed Disk (60blades and 10 packets)

Three different modal analyses were performed to estimate natural frequencies and associated mode shapes. For the first analysis, a disk with single continuous shroud band, i.e., one packet was considered. The second analysis was conducted for an individual bladed disk with individual shroud on the tip of each blade. Essentially, this is the case of 60 packets with only one blade in a packet. Finally, the third analysis was performed for 10 packets with 6 blades in a packet.

Fig. 78 through Fig 80 display plots of 3ND mode shapes for these three cases. The mode shapes for continuous shroud and for free standing blades show a regular sinusoidal form while the mode shape for the 10 packet case looks like a sinusoidal form but it has some irregularities. Fourier analysis of this form yielded the third harmonic as a major contributor, but it also contained some other harmonics. It has been observed in such cases that low order modes do not seem to deviate much from the primary shape; however, for high order modes the deviation is considerable. High order modes appear to have many harmonics other than the expected primary harmonic.

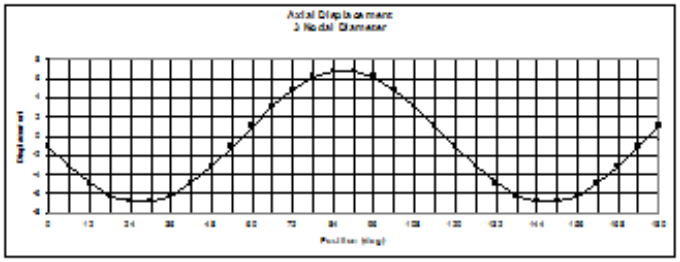

Figure 78 3ND Mode Shape for Single Continuous Shroud

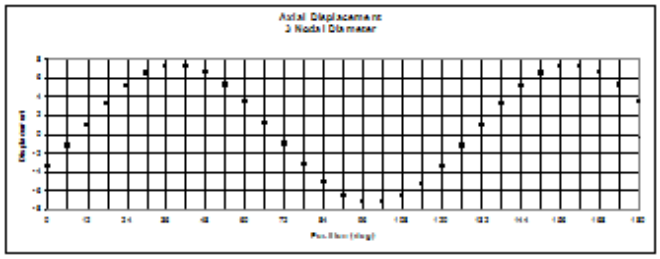

Figure 79 3ND Mode Shape for Blades with Individual Shroud

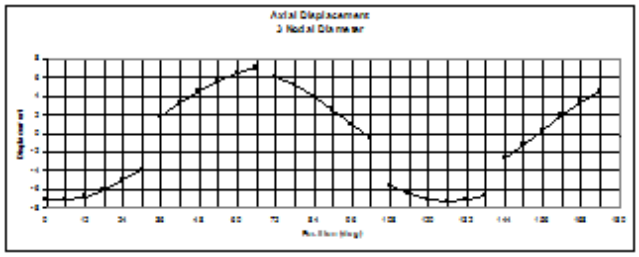

Figure 80 3ND Mode Shape for 10 Packets, 6 Blades in a Packet

Mode shapes for 13ND for these three cases are shown (Fig. 81 thru Fig 83). As expected, the forms for the continuous

and individual blade cases have pure sinusoidal forms, but for the packeted case it is far from pure sinusoidal. For the packeted bladed case, it was found that 13th harmonic was predominant but there was contribution from other harmonics.

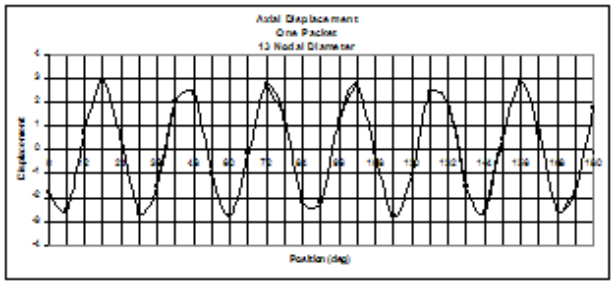


Figure 81 13ND Mode Shape for Single Packet

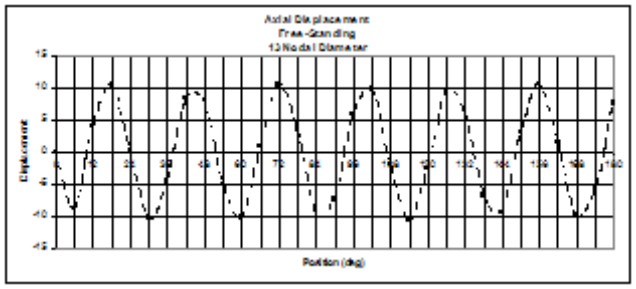


Figure 82 13ND Mode Shape for Individually Shrouded Blades

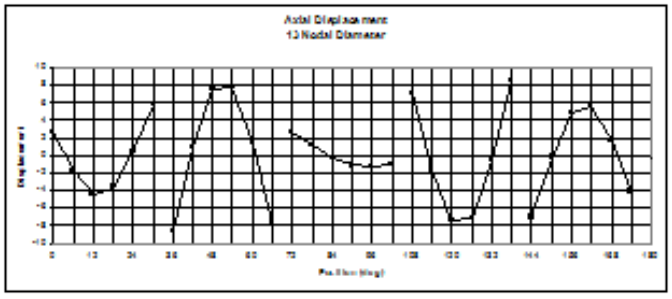


Figure 83 13ND Mode Shape for 10 Blades Packets, 6 Blades in a Packet

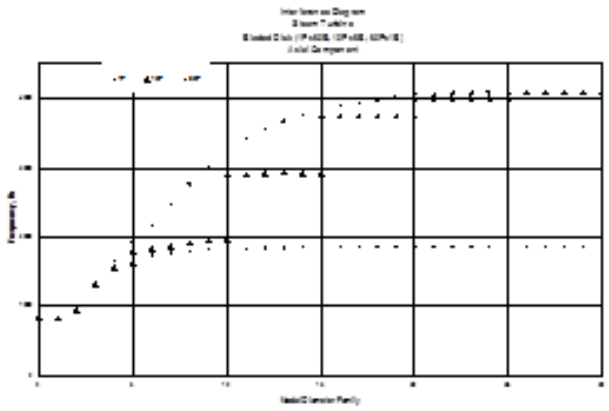

Figure 84 Safe diagram for Single Packet, Individual Blades and 10 Blades Packets, 6 Blades in a Packet

Results of these three cases have been plotted on the Safe diagram as shown in Fig. 84.

The following observations should be mentioned:

1. The frequencies for the completely shrouded blades case are the largest for every mode shape.
2. The frequencies for the individually shrouded blades case are the lowest for every mode shape.
3. The frequencies for the packeted blades case fall in between these two limits.
4. The 5ND, 10ND, 15ND, 20ND and 25ND modes for the packet case have split in two frequencies.
5. The displacement patterns of the blades within a packet are quite different between these modes.
6. For example, for the 10ND, the first mode shows axial-U type displacement while the second one displays axial-S type displacement.
7. The response of blades in these two cases is expected to be different.

To determine the harmonic contents of any mode shape a Fourier analysis utilizing the displacement values of the blade obtained from the modal analysis should be performed. It is a tedious task but an approximate method that has been developed using spring-mass system by observing results of many simple analyses can be used. This method identifies harmonics that will participate in a particular mode for a given construction. However, it does not provide the actual relative contribution of each harmonics.

Singh and Lucas (2011) have explained a graphical method to estimate participation of harmonics for any mode for packeted bladed disc. They also provided mathematical expression to arrive at similar results.

After numerous analyses for packeted bladed disk a mathematical relationship was developed for any mode for any construction.

M nodal diameter mode shape may be written as a general expression given below, where L is the number of harmonic contents.

$$X(M) = \Sigma A_l \sin(L\theta + \varphi_L) \quad (9)$$

The mode shape for M nodal diameter in a general case for packeted bladed disk was found to follow the following expression. The harmonic content, L, can be estimated as follows for the packeted bladed disk:

$$L = \text{abs}(l.n \pm M) \quad (10)$$

Where $l = 0,1,2,3,4,\ldots$
$n$ = number of packets
$N$ = number of blades

and

$$0 \leq L \leq N \text{ or } (N-1)/2 \text{ if } N \text{ is an odd number} \quad (11)$$

A simple way of examining the effect of impurity in mode shape and the shape of the aerodynamic forces can be done by estimating work done by the forces during the motion of a particular mode shape. Figure 85 is the plot of 13 ND mode shape of a packeted bladed disk. Number of blades is 60 and number of packets is 10 with 6 blades in a packet. The largest harmonic content of the shape is thirteenth but there are other harmonics. The harmonic contents of this mode can be estimated by using equation 10.

For this case,
n = 10
M = 13
N = 60
L = abs (l. (10) ± 13)
For l = 0, L = 13
For l = 1, L = 23 and 3
For l = 2, L = 33 and 7
For l = 3, L = 43 and 17
For l = 4, L = 53 and 27
For l = 5, L = 63 and 37

The harmonic contents should be less than 30 (N/2 = 60/2 = 30) according to equation 15, therefore, the expected harmonic contents for this mode are 3, 7, 13, 17 and 27.

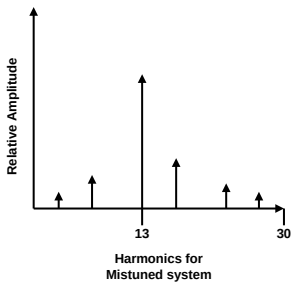


Figure 85 Estimated Harmonic Content in 13ND for 10 Packets

***Expression for work done for structure mistuned bladed disk***

The general expression for the mode shape and the general expression for mistuned forcing with development of work done are provided in the Appendix. The actual relative magnitude of the coefficients for mode shape and forcing should be estimated by performing a Fourier analysis.

Using the complete integral relationship, the final expression of work done is given by the following:

$$\int_0^{2\pi} dW = \pi (7A_7F_7 \cos\varphi_7 \cos\phi_7 + 13A_{13} F_{13} \cos\varphi_{13} \cos\phi_{13}) \quad (12)$$

*Summary*

1. The blade will respond to the harmonics of force that match with the harmonic contents of the mode shape.
2. The resulting response distribution will be different than the mode shape.
3. It is quite possible that there will not be a true resonance, but a forced response in such a situation.

**CONCLUSIONS**

1. For pure resonance to occur, the frequency of the exciting force must equal the natural frequency of vibration, and the profile (shape) of the applied force must be the same shape as the mode shape associated with that natural frequency (true for tuned and mistuned system).
2. For a tuned (structural and forcing) system above conditions are met and the response of the system is very high. Magnitude of response depends on the damping.
3. In the general case of mistuned system (random or deliberate), the blade will respond to the harmonics of force that match with the harmonic contents of the mode shape. The resulting response distribution may be different than the mode shape. It is quite possible that there will not be a true resonance, but a forced response in such a situation.
4. Safe diagram is used for both types of system.
5. The phenomenon of split frequencies has been demonstrated and plotted on the Safe diagram for evaluation. This has been pronounced and very clear for packeted bladed disc construction.

## APPENDIX

## EXPRESSION FOR WORK DONE FOR A TUNED BLADED DISK

The general expression for the mode shape can be written as

$$X(M) = \Sigma A_L \sin(L\theta + \varphi_L) \quad \text{(A1)}$$

Where L is the half of the number of blades (N) for even number of blades or (N-1)/2 for odd number of blades on the disk

$$\begin{aligned} X(M) &= A_0+A_1\sin(\theta+\varphi_1)+A_2\sin(2\theta+\varphi_2)+A_3\sin(3\theta+\varphi_3) \\ &\quad +\ldots\ldots\ldots\ldots+A_L\sin(L\theta+\varphi_L) \\ &= A_0+A_1(\sin\theta\cos\varphi_1+\cos\theta\sin\varphi_1) \\ &\quad +A_2(\sin2\theta\cos\varphi_2+\cos2\theta\sin\varphi_2) \\ &\quad +A_3(\sin3\theta\cos\varphi_3+\cos3\theta\sin\varphi_3) \\ &\quad +\ldots\ldots\ldots+A_L(\sin L\theta\cos\varphi_L+\cos L\theta\sin\varphi_L) \quad \text{(A2)} \end{aligned}$$

In general case when forcing is also mistuned then the shape of the force can be expressed as follows:

$$\begin{aligned} F(N) &= F_0+F_1\cos(\theta+\phi_1)+F_2\cos(2\theta+\phi_2)+ \\ &\quad F_3\cos(3\theta+\phi_3)+\ldots\ldots\ldots+F_L\cos(L\theta+\phi_L) \\ &= F_0+F_1(\cos\theta\cos\phi_1-\sin\theta\sin\phi_1) \\ &\quad +F_2(\cos2\theta\cos\phi_2-\sin2\theta\sin\phi_2) \\ &\quad +F_3(\cos3\theta\cos\phi_3-\sin3\theta\sin\phi_3)+\ldots\ldots\ldots \\ &\quad +F_L(\cos L\theta\cos\phi_L-\sin L\theta\sin\phi_L) \quad \text{(A3)} \end{aligned}$$

$$dW = F(N).d(X(M))$$

$$\begin{aligned} d(X(M)) &= (A_0+A_1(\cos\theta\cos\varphi_1-\sin\theta\sin\varphi_1) \\ &\quad +2A_2(\cos2\theta\cos\varphi_2-\sin2\theta\sin\varphi_2) \\ &\quad +3A_3(\cos3\theta\cos\varphi_3-\sin3\theta\sin\varphi_3) \\ &\quad +\ldots\ldots\ldots \\ &\quad +LA_L(\cos L\theta\cos\varphi_L-\sin L\theta\sin\varphi_L))\,d\theta \quad \text{(A4)} \end{aligned}$$

$$\begin{aligned} dW &= (F_0+F_1(\cos\theta\cos\phi_1-\sin\theta\sin\phi_1) \\ &\quad +F_2(\cos2\theta\cos\phi_2-\sin2\theta\sin\phi_2) \\ &\quad +F_3(\cos3\theta\cos\phi_3-\sin3\theta\sin\phi_3)+\ldots\ldots\ldots \\ &\quad +F_L(\cos L\theta\cos\phi_L-\sin L\theta\sin\phi_L)) \\ &\quad x(A_0+A_1(\cos\theta\cos\varphi_1-\sin\theta\sin\varphi_1) \\ &\quad +2A_2(\cos2\theta\cos\varphi_2-\sin2\theta\sin\varphi_2) \\ &\quad +3A_3(\cos3\theta\cos\varphi_3-\sin3\theta\sin\varphi_3) \\ &\quad +\ldots\ldots\ldots \\ &\quad +LA_L(\cos L\theta\cos\varphi_L-\sin L\theta\sin\varphi_L))\,d\theta \quad \text{(A5)} \end{aligned}$$

Finally, the work done, W, is given by

$$\begin{aligned} \int_0^{2\pi} \mathbf{dW} &= \int_0^{2\pi} ((F_0+F_1(\cos\theta\cos\phi_1-\sin\theta\sin\phi_1) \\ &\quad +F_2(\cos2\theta\cos\phi_2-\sin2\theta\sin\phi_2) \\ &\quad +F_3(\cos3\theta\cos\phi_3-\sin3\theta\sin\phi_3)+\ldots\ldots\ldots \\ &\quad +F_L(\cos L\theta\cos\phi_L-\sin L\theta\sin\phi_L)) \\ &\quad x(A_0+A_1(\cos\theta\cos\varphi_1-\sin\theta\sin\varphi_1) \\ &\quad +2A_2(\cos2\theta\cos\varphi_2-\sin2\theta\sin\varphi_2) \\ &\quad +3A_3(\cos3\theta\cos\varphi_3-\sin3\theta\sin\varphi_3) \\ &\quad +\ldots\ldots\ldots \\ &\quad +LA_L(\cos L\theta\cos\varphi_L-\sin L\theta\sin\varphi_L)))\,d\theta \quad \text{(A6)} \end{aligned}$$

$$\begin{aligned} W &= \int_0^{2\pi} A_0F_0\,d\theta + \int_0^{2\pi} A_1F_1\cos\varphi_1\cos\phi_1\cos^2(\theta)\,d\theta \\ &\quad + \int_0^{2\pi} 2A_2F_2\cos\varphi_2\cos\phi_2\cos^2(2\theta)\,d\theta \\ &\quad + \int_0^{2\pi} 3A_3F_3\cos\varphi_3\cos\phi_3\cos^2(3\theta)\,d\theta \\ &\quad + \ldots\ldots\ldots\ldots\ldots\ldots\ldots\ldots\ldots\ldots \\ &\quad + \int_0^{2\pi} LA_LF_L\cos\varphi_L\cos\phi_L\cos^2(L\theta)\,d\theta \end{aligned}$$

Using the complete integral relationship, equation 11 reduces to the following:

$$\begin{aligned} W = \pi\,(&2A_0F_0+A_1F_1\cos\varphi_1\cos\phi_1+2A_2F_2\cos\varphi_2\cos\phi_2 \\ &+3A_3F_3\cos\varphi_3\cos\phi_3+\ldots\ldots\ldots \\ &+LA_LF_L\cos\varphi_L\cos\phi_L) \quad \text{(A7)} \end{aligned}$$

## EXPRESSION FOR WORK DONE FOR STRUCTURE MISTUNED BLADED DISK

The general expression for the mode shape can be written as

$$\begin{aligned} X(M) &= A_3\sin(3\theta+\varphi_3)+A_7\sin(7\theta+\varphi_7)+A_{13}\sin(13\theta+\varphi_{13}) \\ &\quad +A_{17}\sin(17\theta+\varphi_{17})+A_{23}\sin(23\theta+\varphi_{23})+A_{27}\sin(27\theta+\varphi_{27}) \\ &= A_3(\sin3\theta\cos\varphi_3+\cos3\theta\sin\varphi_3) \\ &\quad +A_7(\sin7\theta\cos\varphi_7+\cos7\theta\sin\varphi_7) \\ &\quad +A_{13}(\sin13\theta\cos\varphi_{13}+\cos13\theta\sin\varphi_{13}) \\ &\quad +A_{17}(\sin17\theta\cos\varphi_{17}+\cos17\theta\sin\varphi_{17}) \\ &\quad +A_{23}(\sin23\theta\cos\varphi_{23}+\cos23\theta\sin\varphi_{23}) \\ &\quad +A_{27}(\sin27\theta\cos\varphi_{27}+\cos27\theta\sin\varphi_{27}) \quad \text{(A8)} \end{aligned}$$

The actual relative magnitude of the coefficients should be estimated by performing a Fourier analysis.

In general case when forcing is also mistuned then the shape of the force can be expressed as follows:

$$\begin{aligned} F(N) &= F_0+F_4\cos(4\theta+\phi_4)+F_7\cos(7\theta+\phi_7)+ \\ &\quad F_{13}\cos(13\theta+\phi_{13})+F_{14}\cos(14\theta+\phi_{14})+ \\ &\quad F_{24}\cos(24\theta+\phi_{24})+F_{28}\cos(28\theta+\phi_{28}) \\ &= F0+F_4\,(\cos4\theta\cos\phi_4-\sin4\theta\sin\phi_4) \\ &\quad +F_7\,(\cos7\theta\cos\phi_7-\sin7\theta\sin\phi_7) \\ &\quad +F_{13}\,(\cos13\theta\cos\phi_{13}-\sin13\theta\sin\phi_{13}) \\ &\quad +F_{14}\,(\cos14\theta\cos\phi_{14}-\sin14\theta\sin\phi_{14}) \\ &\quad +F_{24}\,(\cos24\theta\cos\phi_{24}-\sin24\theta\sin\phi_{24}) \\ &\quad +F_{28}\,(\cos28\theta\cos\phi_{28}-\sin28\theta\sin\phi_{28}) \qquad (A9) \end{aligned}$$

$$dW = F(N).d(X(M))$$

$$\begin{aligned} d(X(M)) &= (3A_3(\cos3\theta\cos\varphi_3-\sin3\theta\sin\varphi_3) \\ &\quad +7A_7\,(\cos7\theta\cos\varphi_7-\sin7\theta\sin\varphi_7) \\ &\quad +13A_{13}\,(\cos13\theta\cos\varphi_{13}-\sin13\theta\sin\varphi_{13}) \\ &\quad +17A_{17}\,(\cos17\theta\cos\varphi_{17}-\sin17\theta\sin\varphi_{17}) \\ &\quad +23A_{23}\,(\cos23\theta\cos\varphi_{23}-\sin23\theta\sin\varphi_{23}) \\ &\quad +27A_{27}\,(\cos27\theta\cos\varphi_{27}-\sin27\theta\sin\varphi_{27}))\,d\theta \qquad (A10) \end{aligned}$$

$$\begin{aligned} dW &= (F_0+F_4\,(\cos4\theta\cos\phi_4 \\ &\quad -\sin4\theta\sin\phi_4)+F_7\,(\cos7\theta\cos\phi_7-\sin7\theta\sin\phi_7) \\ &\quad +F_{13}\,(\cos13\theta\cos\phi_{13}-\sin13\theta\sin\phi_{13}) \\ &\quad +F_{14}\,(\cos14\theta\cos\phi_{14}-\sin14\theta\sin\phi_{14}) \\ &\quad +F_{24}\,(\cos24\theta\cos\phi_{24}-\sin24\theta\sin\phi_{24}) \\ &\quad +F_{28}\,(\cos28\theta\cos\phi_{28}-\sin28\theta\sin\phi_{28})) \\ &\quad \times(3A_3\,(\cos3\theta\cos\varphi_3-\sin3\theta\sin\varphi_3) \\ &\quad +7A_7(\cos7\theta\cos\varphi_7-\sin7\theta\sin\varphi_7) \\ &\quad +13A_{13}\,(\cos13\theta\cos\varphi_{13}-\sin13\theta\sin\varphi_{13}) \\ &\quad +17A_{17}\,(\cos17\theta\cos\varphi_{17}-\sin17\theta\sin\varphi_{17}) \\ &\quad +23A_{23}\,(\cos23\theta\cos\varphi_{23}-\sin23\theta\sin\varphi_{23}) \\ &\quad +27A_{27}\,(\cos27\theta\cos\varphi_{27}-\sin27\theta\sin\varphi_{27}))\,d\theta \qquad (A11) \end{aligned}$$

$$\begin{aligned} \int_0^{2\pi} dW &= \int_0^{2\pi} (F_0+F_4\,(\cos4\theta\cos\phi_4\sin4\theta\sin\phi_4) \\ &\quad +F_7\,(\cos7\theta\cos\phi_7-\sin7\theta\sin\phi_7) \\ &\quad +F_{13}\,(\cos13\theta\cos\phi_{13}-\sin13\theta\sin\phi_{13}) \\ &\quad +F_{14}\,(\cos14\theta\cos\phi_{14}-\sin14\theta\sin\phi_{14}) \\ &\quad +F_{24}\,(\cos24\theta\cos\phi_{24}-\sin24\theta\sin\phi_{24}) \\ &\quad +F_{28}\,(\cos28\theta\cos\phi_{28}-\sin28\theta\sin\phi_{28})) \\ &\quad \times(3A_3\,(\cos3\theta\cos\varphi_3-\sin3\theta\sin\varphi_3) \\ &\quad +7A_7(\cos7\theta\cos\varphi_7-\sin7\theta\sin\varphi_7) \\ &\quad +13A_{13}\,(\cos13\theta\cos\varphi_{13}-\sin13\theta\sin\varphi_{13}) \\ &\quad +17A_{17}\,(\cos17\theta\cos\varphi_{17}-\sin17\theta\sin\varphi_{17}) \\ &\quad +23A_{23}\,(\cos23\theta\cos\varphi_{23}-\sin23\theta\sin\varphi_{23}) \\ &\quad +27A_{27}\,(\cos27\theta\cos\varphi_{27}-\sin27\theta\sin\varphi_{27}))\,d\theta \qquad (A12) \end{aligned}$$

Using the complete integral relationship, equation 20 reduces to the following:

$$\begin{aligned} \int_0^{2\pi} dW &= \int_0^{2\pi} 7A_7F_7\cos\varphi_7\cos\phi_7\cos^2(7\theta)\,d\theta \\ &\quad +\int_0^{2\pi} 13A_{13}F_{13}\cos\varphi_{13}\cos\phi_{13}\cos^2(13\theta)\,d\theta \\ &= \pi\,(7A_7F_7\cos\varphi_7\cos\phi_7 \\ &\quad +13A_{13}F_{13}\cos\varphi_{13}\cos\phi_{13}) \qquad (A13) \end{aligned}$$

## REFERENCES


Campbell, W, 1924, "The Protection of Steam-Turbine Disk Wheels from Axial Vibration," Trans ASME, Vol. 46, pp 31-160.

Ewins, D.J. 1969. "The Effects of Detuning Upon the Forced Vibrations of Bladed Disk." Journal of Sound and Vibration. Vol. 9(1). Pp.65-79.

Ewins, D.J. 1970. "A Study of Resonance Coincidence in Bladed Discs," Journal of Mechanical Engineering Science, 12, (5).

Ewins, D.J. 1973,"Vibrational Characteristics of Bladed Disk Assemblies,", Journal of Mechanical Engineering Science, 15, (3), 1973.

Ewins, D.J., 1976,"Studies to Gain Insight into the Complexities of Blade Vibration Phenomena," Conference on Vibration in Rotating Machinery, ImechE, C184/76, pp 165-172.

Johnson, D.C. and Bishop, R.E.D., 1956, "The Modes of Vibration of a Certain System Having a Number of Equal Frequencies," Journal of Applied Mechanics, Transaction of ASME, September, pp 379-384.

Nelson, W. E., 1979, "Maintenance Techniques for Turbomachinery," Proceedings of the 8th Turbomachinery Symposium,Turbomachinery Laboratory, Texas A & M University, College Station, Texas, pp. 11-20.

Prohl, M. A., (1956),"A Method for Calculating Vibration Frequency and Stress of a Banded Group of Turbine Blades," Trans ASME, Paper No. 56-A-116.

Provanzale, G.E., and Skok, M.W. 1973, "A Cure for Steam Turbine Blade Failure," ASME Paper No.73-PET-71.

Singh, M. and Schiffer, D., 1982. "Vibrational Characteristic of Packeted Bladed Disc," Presented at ASME Design Engineering Technical Conf., Washington, DC, September. 82-DET-137.

Singh, M. P., Vargo, J. J., Schiffer, D. M. and Dello, J. D., 1988, "Safe Diagram – A Design Reliability Tool for Turbine Blading," Proceedings of the 17th Turbomachinery Symposium, Turbomachinery Laboratory, Texas A & M University, College Station, Texas, pp. 93-101.

Singh, M.P. and Ewins, D.J., 1988. "A Probabilistic Analysis of a Mistuned Bladed Turbine Disc," ImechE Conference, Edinburgh, UK, C229/88.

Singh, M. P. and Vargo, J.J. 1989."Reliability Evaluation of Shrouded Blading Using the SAFE Interference Diagram," J. J., Journal of Engineering for Gas Turbine and Power, vol. 111, pp. 601-609.

Singh, M.P. 1992. "Predicting the Randomness of Forced Vibration Response of a Bladed Disc," ImechE Conference, Bath, UK, C432/128.

Singh, M, Thakur, B, Sullivan, W. and Donald, G., 2003, "Resonance Identification for Impellers," Proceedings of the 32nd Turbo Symposium, Texas A&M University, College Station, Texas 77840-3123.

Singh, M.P., Cencula, James. E, Wu, Randy, Ho, James and Higgins, Ernie, 2007, "Successful Solution to a Turbo-expander Wheel Failure, Operating in an Erosive Environment of Geothermal Steam," Proceeding of MEMEC, Bahrain, November 4-7, Paper # 07-438.

Singh, M.P. and Drosjack, M, 2008, "Emerging Advanced Technologies to Assess Reliability of Industrial Steam Turbine Blade Design," Proceedings of the 37th Turbomachinery Symposium, Turbomachinery Laboratory, Texas A&M University, College Station, Texas, pp 169-188.

Singh, Murari and Lucas, George, 2011, "*Blade Design and Analysis*," McGraw-Hill, New York.

Weaver, F. and Prohl, M. 1956, "High Frequency Vibration of Steam Turbine Buckets, ASME Paper No. 56-A-119.

## ACKNOWLEDGEMENTS

Thanks to many researchers who have published papers on the subject. Special thanks to many of my coworkers and friends who helped me to continuously improve the topic. Some of them are Late Howard Vreeland, Don Schiffer, Jim Dello, John Vargo, Bill Sullivan, Bhabesh Thakur, Terryl Mathews, Mike Drosjack, Cyrus Meher-Homji, Late Cliff Cook, David Ewins and James Cencula.